RESEARCH ARTICLE

Journal of Cellular Biochemistry WILEY

Disruption of the MICOS complex leads to an aberrant cristae structure and an unexpected, pronounced lifespan extension in *Podospora anserina*

Verena Warnsmann[1] | Lisa-Marie Marschall[1] | Anja C. Meeßen[1] |
Maike Wolters[1] | Lea Schürmanns[1] | Marion Basoglu[2] | Stefan Eimer[2] |
Heinz D. Osiewacz[1]

[1]Institute of Molecular Biosciences, Faculty of Biosciences, Goethe-University, Frankfurt, Germany

[2]Institute for Cell Biology and Neuroscience, Faculty of Biosciences, Goethe-University, Frankfurt, Germany

Correspondence
Heinz D. Osiewacz, Institute of Molecular Biosciences, Faculty of Biosciences, Goethe-University, Max-von-Laue-Str. 9, Frankfurt 60438, Germany.
Email: osiewacz@bio.uni-frankfurt.de

Abstract

Mitochondria are dynamic eukaryotic organelles involved in a variety of essential cellular processes including the generation of adenosine triphosphate (ATP) and reactive oxygen species as well as in the control of apoptosis and autophagy. Impairments of mitochondrial functions lead to aging and disease. Previous work with the ascomycete *Podospora anserina* demonstrated that mitochondrial morphotype as well as mitochondrial ultrastructure change during aging. The latter goes along with an age-dependent reorganization of the inner mitochondrial membrane leading to a change from lamellar cristae to vesicular structures. Particularly from studies with yeast, it is known that besides the F_1F_o-ATP-synthase and the phospholipid cardiolipin also the "mitochondrial contact site and cristae organizing system" (MICOS) complex, existing of the Mic60- and Mic10-subcomplex, is essential for proper cristae formation. In the present study, we aimed to understand the mechanistic basis of age-related changes in the mitochondrial ultrastructure. We observed that MICOS subunits are coregulated at the posttranscriptional level. This regulation partially depends on the mitochondrial iAAA-protease PaIAP. Most surprisingly, we made the counterintuitive observation that, despite the loss of lamellar cristae and of mitochondrial impairments, the ablation of MICOS subunits (except for PaMIC12) leads to a pronounced lifespan extension. Moreover, simultaneous ablation of subunits of both MICOS subcomplexes synergistically increases lifespan, providing formal genetic evidence that both subcomplexes affect lifespan by different and at least partially independent pathways. At the molecular level, we found that ablation of Mic10-subcomplex components leads to a mitohormesis-induced lifespan extension, while lifespan extension of Mic60-subcomplex mutants seems to be controlled by pathways involved in the control of phospholipid homeostasis. Overall, our

data demonstrate that both MICOS subcomplexes have different functions and play distinct roles in the aging process of *P. anserina*.

KEYWORDS

aging, cristae, MICOS, mitochondria, mitohormesis, *Podospora anserina*

1 | INTRODUCTION

Mitochondria are double-membrane-bound, ubiquitous eukaryotic organelles with a variety of essential functions. They play a central role in organismal aging and human diseases.[1–5] The inner mitochondrial membrane forms invaginations, the so-called cristae. At their basis, cristae junctions connect the cristae membrane with the inner boundary membrane, the part of the inner membrane which is closely apposed to the outer membrane.[6–8] This characteristic architecture is crucial for mitochondrial function.[9]

Cristae morphology is highly variable and was found to change during aging in various organisms and in numerous human disorders.[10] For instance, in the filamentous fungus *Podospora anserina*, a well-established aging model with a strong mitochondrial etiology of aging, functional mitochondria from young individuals contain lamellar cristae whereas mitochondria from older cultures lose this typical cristae structure and the inner membrane forms vesicles.[11] The formation and maintenance of cristae are mediated by the interplay of two major protein complexes and the mitochondrial phospholipid cardiolipin.[7,12–14] The first complex is the dimeric F_1F_o-ATP-synthase, which is required for the positive curvature at the cristae tips.[15–17] Loss of F_1F_o-ATP-synthase dimers leads to aberrant cristae structures.[18–21] For instance, in *P. anserina* the loss of F_1F_o-ATP-synthase dimers causes the loss of lamellar cristae and a mitophagy-dependent reduction of lifespan.[21,22]

The second protein complex is the evolutionary conserved "mitochondrial contact site and cristae organizing system" (MICOS) complex. This complex is responsible for negative membrane curvature at the base of cristae, for cristae junction formation as well as connections of the inner and outer mitochondrial membrane.[23–26] The MICOS complex is composed of several subunits. In the budding yeast, MICOS contains six subunits, which are organized in two subcomplexes, a Mic60- and a Mic10-subcomplex (Figure 1A). The Mic60-subcomplex consists of the core-subunit MIC60 and the regulatory subunit MIC19 and connects the inner and outer mitochondrial membranes. The Mic10-subcomplex of yeast is composed of the core-subunit MIC10 and the regulatory subunits MIC26, MIC27, and MIC12. Oligomerization of MIC10 monomers initiates membrane curvature at cristae junctions. In the human

MICOS complex, the Mic60-subcomplex contains MIC25 as an additional subunit. Furthermore, instead of MIC12, MIC13/QIL1 is part of the human Mic10-subcomplex. The loss of individual MICOS subunits causes a disruption of cristae junctions combined with aberrant cristae structure.[27–29]

Both cristae-forming protein complexes, F_1F_o-ATP-synthase dimers, and the MICOS complex are stabilized by the mitochondrial phospholipid cardiolipin, which promotes cristae formation.[13,24,30,31] Moreover, due to the cone-shaped structure, cardiolipin itself is involved in cristae curvature formation.[32,33] In yeast, plants and flies mutants lacking cardiolipin synthase (CRD1) or the cardiolipin remodeling enzyme tafazzin (TAZ1) cristae structure is abnormal.[30,34–39] Similar to impairments in F_1F_o-ATP-synthase dimerization, ablation of CRD1 leads to lifespan reduction in *Drosophila melanogaster* and *P. anserina*.[30,40]

Although the structure of MICOS and its importance for the mitochondrial ultrastructure are well studied in yeast and human, the functional impact of MICOS impairments on the aging process remains unclear. For *P. anserina*, a previously published model postulates that the MICOS complex has to dissociate during aging to allow the transition from tubular to vesicular inner membrane organization.[11] In the current study, we set out to experimentally address this process in more detail. First, we identified homologs to the yeast MICOS subunits in *P. anserina* and analyzed their regulation and impact on organismic aging. We demonstrate that the steady-state levels of identified MICOS subunits in *P. anserina* are coregulated, and this regulation is partially dependent on mitochondrial iAAA-protease PaIAP. Surprisingly, we made the counterintuitive observation that, despite the defect of cristae junction formation, the ablation of MICOS subunits leads to a pronounced lifespan extension. So far, the MICOS complex was thought to act as a unit. However, in contrast here we demonstrate that the MICOS complex rather acts as two subcomplexes that both regulate lifespan through different pathways. In Mic10-subcomplex mutants, the lifespan extension results from the induction of mitohormesis, which does not appear to play a major role in the lifespan extension of Mic60-subcomplex mutants.
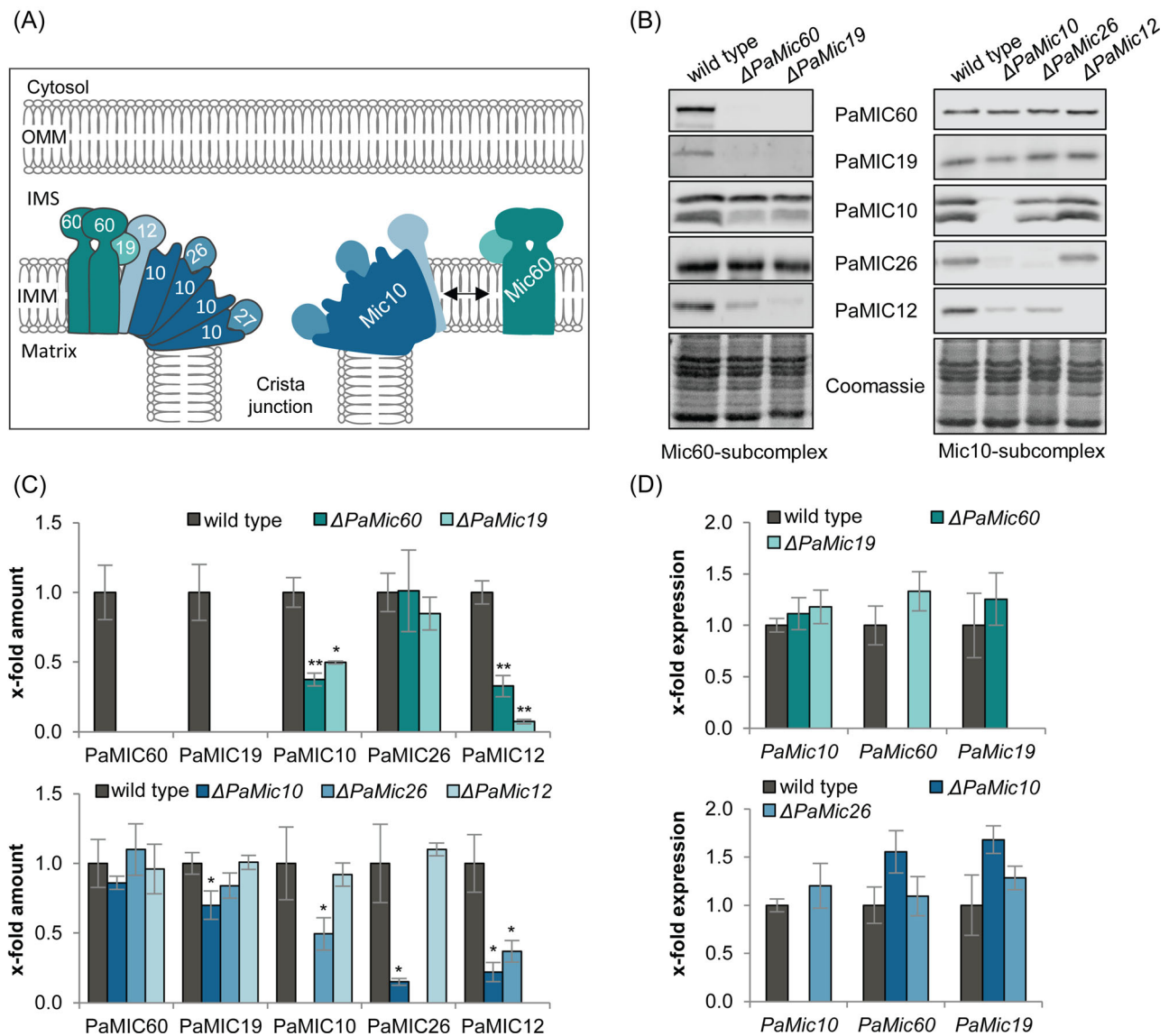
FIGURE 1 MICOS subunits affect each other. (A) Scheme depicting the MICOS subcomplexes and the individual subunits in yeast. The Mic60-subcomplex consists of the subunits MIC60 and MIC19. MIC10, MIC27, MIC26, and MIC12 form the Mic10-subcomplex. Together both subcomplexes form the MICOS complex. IMM, inner mitochondrial membrane; IMS, intermembrane space; OMM, outer mitochondrial membrane. (B) Western blot analysis of mitochondrial protein extracts of *Podospora anserina* wild type, *ΔPaMic60*, *ΔPaMic19*, *ΔPaMic10*, *ΔPaMic26*, and *ΔPaMic12* using antibodies against the indicated proteins. (C) Quantification of MICOS protein abundance normalized to the Coomassie-stained gel and related to the wild type (set to 1). Data are mean abundance ± SD (every three biological replicates). (D) Relative transcript levels of *PaMic10*, *PaMic60*, and *PaMic19* in wild type, *ΔPaMic60*, *ΔPaMic19*, and wild type, *ΔPaMic10* and *ΔPaMic26* (every three biological replicates). Transcript levels of wild-type cultures were set to 1. Data are mean expression ± SD. *Significant differences to wild type; *$p < 0.05$; **$p < 0.01$. MICOS, mitochondrial contact site and cristae organizing system.

2 | MATERIALS AND METHODS

2.1 | *P. anserina* strains and cultivation

In this study, the *P. anserina* wild-type strain "s,"[41] *PaSod3H26L::Gfp*,[42] *ΔPaIap*[43] as well as the newly generated mutants *ΔPaMic60*, *ΔPaMic19*, *ΔPaMic10*, *ΔPaMic26*, *ΔPaMic12*, *ΔPaMic60/ΔPaIap*, *ΔPaMic10/ΔPaIap*, *ΔPaM ic26/ΔPaIap*, *ΔPaMic60/PaSod3H26L::Gfp*, *ΔPaMic19/ PaSod3H26L::Gfp*, *ΔPaMic10/PaSod3H26L::Gfp*, *ΔPaMic26/ PaSod3H26L::Gfp*, and *ΔPaMic12/PaSod3H26L::Gfp* were used. Strains were grown on standard cornmeal agar (BMM: "Biomalz-Mais" Medium) at 27°C under constant light.[44] For spore germination BMM with 60 mM ammonium acetate (Merck; 1116.1000) was used. Spores were incubated at 27°C in the dark for 2 days. All strains

used in this study were derived from monokaryotic ascospores.[44]

2.2 | Cloning procedures and generation of *P. anserina* mutants

All transgenic strains are in the genetic background of wild-type strain "s." MICOS deletions strains were generated according to a method developed by El-Khoury et al.[45] using the plasmid pKO7 and the strain *ΔPaKu70*.[46] In short, approximately 1 kbp long fragments corresponding to the 5′ and 3′ flanking regions of the respective gene of interest were amplified by PCR using sequence-specific oligonucleotides (Supporting Information: Table S1) with appropriate restriction site overhangs and cloned into the plasmid pKO7 to flank a hygromycin B-resistance gene. For deletion of *PaMic26*, *PaMic12*, and *PaMic19* a cloning strategy with the restriction sites ClaI and HindIII (5′-region) and PstI and BamHI (3′-region) was used. In the case of *PaMic10* and *PaMic60*, different cloning strategies were used. The 5′-regions were cloned with the restrictions sites BamHI and PstI (*PaMic60*) or KpnI and HindIII (*PaMic10*). For cloning of 3′-regions the restriction enzymes EcoRV and HindIII (*PaMic60*) or PstI and BamHI (*PaMic10*) were used. The resulting gene-specific deletion vectors were used to transform *P. anserina* spheroplasts of the phleomycin-resistant *ΔPaKu70* strain. Several independent primary transformants were selected by their hygromycin B-resistance and crossed with the wild type to reintroduce the *PaKu70* gene. Hygromycin B-resistant and phleomycin-sensitive offspring were verified by Southern blot analysis. Afterward, the phenotype and lifespan of these independent mutants were analyzed. All of them displayed the same phenotype and were long-lived. Therefore, the progeny of only one primary transformant was selected for all further analyses.

For complementation analysis, MICOS genes with promoter, terminator, and appropriate restriction site overhangs were amplified with specific oligonucleotides (Supporting Information: Table S2) and cloned into the plasmid pKO6 containing a phleomycin resistance cassette.[47] After transformation of the resulting plasmid in spheroplasts of the corresponding deletion strain, selection of transformants was performed by growth on a phleomycin-containing medium.

2.3 | Generation of *P. anserina* double mutants

For double mutant generation, the single mutant strains were crossed with each other. Subsequently, strains were selected from the progeny containing both mutations.

2.4 | Southern blot analysis

DNA isolation was performed according to a well-established protocol from Lecellier and Silar.[48] From each sample 500 ng DNA was digested with EcoRV. DNA digestion, gel electrophoresis, and Southern blotting were carried out by standard protocols. According to the manufacturer's protocol for Southern blot hybridization and detection, digoxigenin-labeled hybridization probes (DIG DNA Labeling and Detection Kit; Roche Applied Science; 11175033910) were used. The phleomycin resistance gene (*Ble*) specific hybridization probe corresponds to the 1293 bp BamHI-fragment of the plasmid pKO4.[49] The 736 bp XhoI-fragment of the plasmid pSM4[50] was used as a specific hybridization probe for the hygromycin resistance gene (*Hyg*). The specific hybridization probes of the MICOS genes were amplified by PCR using gene-specific oligonucleotides (Supporting Information: Table S3).

2.5 | Growth rate and lifespan determination

Determination of the lifespan and the growth rate of *P. anserina* cultures derived from monokaryotic ascospores was performed on M2 medium at 27°C and constant light as previously described.[44] The lifespan of *P. anserina* is defined as the time period in days (d) until growth stops. The growth rate is defined as the distance of growth (cm) of a culture per time period (d).

2.6 | Isolation of total protein extracts

Total protein extracts of *P. anserina* strains were isolated as previously described.[22] Briefly, grown mycelia were homogenized in protein isolation buffer containing 5 mM dithiothreitol (DTT) (Carl Roth; 6908.4) and subsequently sedimented at 9300xg. The supernatant was used as total protein extracts and stored at −20°C.

2.7 | Isolation of mitochondria

For isolation of mitochondria *P. anserina* strains were grown on cellophane foil-covered solid M2 agar for 2 days at 27°C and constant light. Grown mycelial pieces were transferred to a CM-liquid medium and incubated for additional 2 days at 27°C and constant light. The mitochondria of *P. anserina* cultures were isolated according to a published protocol.[51] Afterwards, mitochondria were purified with a discontinuous sucrose gradient (20−36−50%) and ultracentrifugation (100 000xg).[44]

2.8 | Blue native gel electrophoresis (BN-PAGE)

BN-PAGE to separate native protein complexes according to size was performed as described.[52] Briefly, 150 μg of isolated mitochondria were solubilized with digitonin (Sigma-Aldrich; D141) at a detergent/protein ratio of 4 g/g. Solubilized mitochondria were separated on a linear gradient gel (4%−13%) overlaid with a 3.5% stacking gel. After electrophoresis protein complexes were fixed for 30 min in a fixing solution (50% methanol, 10% acetic acid), and subsequently proteins were visualized by 1 h Coomassie staining (0.025% Coomassie blue in 10% acetic acid).

2.9 | Mitochondrial oxygen consumption

Determination of mitochondrial oxygen consumption was performed at 27°C by high-resolution respirometry (Oxygraph-2k series C and G, OROBOROS Instruments). Two hundred milligrams freshly prepared mitochondria were injected into 2 ml air saturated oxygen buffer (0.3 M sucrose, 10 mM KH_2PO_4, 5 mM $MgCl_2$, 1 mM EGTA, 10 mM KCl, and 0.2% BSA; pH 7.2). To promote the ADP-limited complex I-dependent state 4 respiration (state 4) 10 mM pyruvate (Sigma-Aldrich; P2256) and 2 mM malate (Sigma- Aldrich; M1000) were added. Subsequently, 1.5 mM ADP (Sigma-Aldrich; A5285) was added to determine complex I-dependent state 3 respiration (state 3). Data were analyzed using the manufacturer's software DatLab 6.

2.10 | Western blot analysis

Western blot analysis was performed with 50 μg mitochondria or total protein extract as previously described.[22] The following primary antibodies were used: anti-GFP (mouse, 1:10 000 dilution, Sigma-Aldrich; G6795), anti-PaIAP (rabbit, dilution 1:2500, peptide: [H]-KAENQKARFSDVHGC-[OH]; Sigma-Genosy), anti-PaMIC10 (rabbit, dilution 1:10 000, peptide: [H]-AYEEC NSSLKQAAKEIRKQA-[OH]; Davids Biotechnologie GmbH), anti-PaMIC60 (rabbit, dilution 1:10 000, peptide: [H]-KAKKETAALPKVEAKDAALEKK-[OH]; Davids Biotechnologie GmbH), anti-PaMIC19 (rabbit, dilution 1:2000, peptide: [H]-REVEAFKEEVRRVEKGWVEK-[OH]; Davids Biotechnologie GmbH), anti-PaMIC26 (rabbit, dilution 1:10 000, peptide: [H]-PRKPIYDDDLD DPLPTSK-[OH]; Davids Biotechnologie GmbH), anti-PaMIC12 (rabbit, dilution 1:10 000, peptide: [H]-ERAL AERFDQAKRERRLERS-[OH]; Davids Biotechnologie GmbH).

As secondary antibodies, IRDye® 680RD anti-rabbit (goat, 1:15 000 dilution, LIC-OR Biosciences; 926-68071), IRDye® 800CW anti-rabbit (goat, 1:15 000 dilution, LIC-OR Biosciences; 926-32211), and IRDye00 680RD anti-mouse (goat, dilution 1:15 000, LI-COR Biosciences; 926-68070) were used. The Odyssey® Fc imaging system (LIC-OR Biosciences) was used for antibody detection and densitometric quantification was performed with the manufacturer's software image studio (Version 5.2).

2.11 | Quantitative real-time PCR (qRT-PCR)

RNA isolation and cDNA synthesis was performed as previously described.[53] For each strain three biological replicates were analyzed three times each (technical replicates). Transcript levels of PaMic10, PaMic19, and PaMic60 were determined and normalized to the transcript level of PaPorin. The used oligonucleotides are listed in Supporting Information: Table S4. For all genes, PCR efficiency was determined as described.[54]

2.12 | Superoxide and hydrogen peroxide release measurements

For qualitative determination of superoxide anion release from mycelia a histochemical nitro blue tetrazolium (Sigma-Aldrich; N6876) staining was performed as previously described.[55] Analogously, for hydrogen peroxide release a histochemical diaminobenzidine (DAB, Sigma-Aldrich; D-8001) staining was performed as previously described[55]

2.13 | Fluorescence microscopy

P. anserina strains were cultivated on glass slides with a central depression containing 130 μl M2 medium for 1 day under standard conditions. Fluorescence microscopic analyses were performed with the confocal spinning disc Microscope Zeiss Cell Observer SD and a ×63/1.4 oil objective lens (Carl Zeiss Microscopy) using a 488 nm laser line. Image processing was performed with the corresponding software ZEN 2.5 (blue edition).

2.14 | Transmission electron microscopy

For transmission electron microscopy, P. anserina cultures were grown on M2 agar and small agar blocks

were cut out at the 6-day growths front and fixed while shaking for 1 h at room temperature (RT) in 0.1 M cacodylate buffer at pH 7.2 containing 0.25 M sucrose and 4% glutaraldehyde. The fixed samples were then washed two times in 0.1 M cacodylate buffer pH 7.2 containing 10% sucrose at RT. Afterward the samples were stained with 2% OsO_4 for 3 h at RT and washed twice with wash buffer. Before embedding samples were dehydrated by using increasing concentrations of ethanol buffer from 50%, 70%, 90%, and twice 100%, followed by two washes with propylene oxide. Subsequently, samples were embedded in Araldite resin and polymerized. Fifty nanometers thin sections were cut using a Reichert Ultracut ultramicrotome and transferred to coated copper slot grids. Grids were poststained with uranyl acetate and lead citrate and analyzed using a digitalized Zeiss transmission electron microscopy (TEM) 900 operated at 80 keV and equipped with a Troendle 2 K camera.

2.15 | Statistical analysis

Significances of differences in lifespan of individual cultures were statistically analyzed with the IBM SPSS statistics 19 software package (IBM) by generating the Kaplan−Meier survival estimates. We use three independent statistical tests (Breslow [generalized Wilcoxon], log-rank [Mantel−Cox], and the Tarone−Ware) with a pairwise comparison. All other statistical significances were calculated with the Student′s t-test. The corresponding samples were compared with the appropriate wild-type sample. For statistical significance, the minimum threshold was set at $p \leq 0.05$; *$p \leq 0.05$; **$p \leq 0.01$; ***$p \leq 0.001$.

3 | RESULTS AND DISCUSSION

3.1 | Identification of MICOS homologs in *P. anserina*

Various studies from yeast to humans revealed the structure of the MICOS complex and its role in the mitochondrial ultrastructure. Nevertheless, the functional impact of MICOS impairments on the aging process remains unclear. For *P. anserina*, a previously published model postulates that the MICOS complex has to dissociate during aging to allow the age-dependent reorganization of the inner membrane.[11] In the current study, we set out to experimentally address this process in more detail. Since previous studies demonstrated that the MICOS complex is evolutionary conserved,[56] we first performed a protein

BLAST search (http://podospora.i2bc.paris-saclay.fr/blast.php) and identified five homologs of the six yeast MICOS subunits (Table 1, Supporting Information: Figure S1). We termed them PaMIC60, PaMIC19, PaMIC10, PaMIC26, and PaMIC12 in accordance with the published uniform nomenclature.[57] All identified *P. anserina* MICOS subunits possess the typical domains, which are known from yeast and humans (Table 1). For instance, the core subunit PaMIC60 contains a mitofilin domain that is conserved among organisms (Table 1, Supporting Information: Figure S1A). Furthermore, the sequence of PaMIC26 shows the same apolipoprotein-O domain as the corresponding protein in *Saccharomyces cerevisiae* (Table 1). A homolog of the sixth *S. cerevisiae* MICOS subunit MIC27 was not found in *P. anserina*.

3.2 | PaIAP-dependent regulation of MICOS steady-state levels

To experimentally address the question of whether or not the MICOS complex plays a role in *P. anserina* aging, as it was suggested in an earlier study,[11] we generated five *P. anserina* strains each lacking one of the individual MICOS subunits. The corresponding genes were replaced through homologous recombination by a hygromycin resistance cassette. The resulting knockout strains were verified by Southern blot analysis (Supporting Information: Figure S2A). Previous studies in yeast demonstrated that loss of a single MICOS subunit can affect the stability/steady-state levels of the other MICOS subunits, suggesting a coregulation of the MICOS complex subunits.[23,26,31,58] To test whether or not this kind of coregulation also occurs in *P. anserina*, we investigated the steady-state levels of all MICOS subunits in the different *P. anserina* MICOS deletion strains. Indeed, in many cases, either complete loss or severe reduction of the abundance of MICOS subunits occurs in single deletion mutants (Figure 1B,C). In particular, ablation of one of the two Mic60-subcomplex components, PaMIC60 or PaMIC19, leads to the loss of the other subcomplex component. This is similar to the mammalian system where knockdown of *Mic19* leads to the complete loss of Mic60-subcomplex in cell lines.[59,60] In *P. anserina*, proteins of the Mic10-subcomplex are only partially reduced in deletion mutants of the Mic60-subcomplex. In particular, PaMIC10 and PaMIC12 are reduced in both Mic60-subcomplex mutants, whereas PaMIC26 is not affected. Noticeably, two signals were detected with the PaMIC10 antibody which is absent in the *PaMic10* deletion mutant. The upper band probably corresponds to the unprocessed PaMIC10 with mitochondrial targeting sequence at the outside of the mitochondria and the

TABLE 1 Identification of homologs of the *Saccharomyces cerevisiae* MICOS complex in *Podospora anserina*

| MICOS subunit	*S. cerevisiae*	Conserved domain	Putativehomolog in *P.* anserina	Trivial name
MIC60	YKR016W (P36112)	Mitofilin (IPR019133)	Pa_1_1530 (B2A9R4)	PaMIC60
MIC19	YFR011C (P43594)	DUF1690 (IPR012471)	Pa_1_19620 (B2AUM5)	PaMIC19
MIC10	YCL057C-A (Q96VH5)	DUF543 (IPR007512)	Pa_7_7950 (B2AWQ3)	PaMIC10
MIC12	YBR262C (P38341)	AIM5 (IPR031463)	Pa_2_1415 (B2B416)	PaMIC12
MIC26	YGR235C (P50087)	Apolipoprotein-O (IPR019166)	Pa_1_10590 (B2AYB9)	PaMIC26
MIC27	YNL100W (P50945)	No	No	No

Note: Putative homologs were identified in a Blast search or based on domain conservation in the InterPro database using *S. cerevisiae* as a query. UniProt and InterPro accession numbers are provided in brackets. The *P. anserina* MICOS proteins (trivial name) were termed according to the published nomenclature.[57] The numbers correspond to the molecular mass of the proteins.

Abbreviation: MICOS, mitochondrial contact site and cristae organizing system.

lower band reflects PaMIC10 protein after import and processing. Analysis of the Mic10-subcomplex mutants also revealed a strong reduction of Mic10-subcomplex proteins other than those deleted in the mutant and minor effects on the Mic60-subcomplex (Figure 1B,C). For instance, ablation of PaMIC10 led to an almost complete loss of PaMIC26 and PaMIC12 and only slight reductions of the Mic60-subcomplex components PaMIC60 and PaMIC19. Ablation of PaMIC26 reduced the other Mic10-subcomplex components but not those of the Mic60-subcomplex. In contrast, in the *PaMic12* deletion mutant the other MICOS components are not affected (Figure 1B,C). This exception was also described in a yeast *Mic12* deletion strain.[23] Our data suggest that each subcomplex regulates the stability of the other. The loss of one of the two MICOS core-subunit (PaMIC10 or PaMIC60) has the strongest impact on the whole MICOS complex in *P. anserina*. This is in contrast to results from human cells in which only depletion of MIC60, but not MIC10, results in the absence/reduction of all MICOS subunits.[61] In yeast, there are inconsistent data reported. While some studies show that the subcomplexes coregulate each other, others only describe regulation of components of the genetically modified subcomplex and not from the other subcomplex.[23,26,31,58] From our data, we conclude that the five MICOS proteins in *P. anserina* cooperate in an intricate manner and are controlled by a regulatory network.

To analyze at which level the regulation of MICOS proteins takes place, we first investigated the transcript level of selected MICOS genes (Figure 1D). In contrast to protein abundance, transcript levels are not changed in MICOS deletion mutants compared to the wild type. Therefore, regulation must occur at the protein level. From a study with mouse embryonic fibroblasts, it is known, that in *Mic19* knockdown cells the loss of MIC60 is rescued by simultaneous ablation of iAAA protease YME1L[60] suggesting that MICOS components are possible substrates of this protease. To examine this possibility in *P. anserina*, we first analyzed the amount of PaIAP, the *P. anserina* homolog of YME1L, in the MICOS deletion mutants (Figure 2A,B). PaIAP was found to be increased in Mic60-subcomplex mutants but not in Mic10-subcomplex mutants. Thus, the iAAA protease is potentially involved at least in the regulation of Mic60-subcomplex abundance in *P. anserina*. To investigate this possibility in more detail, we generated double mutants which concomitantly lack one MICOS subunit and PaIAP (Supporting Information: Figure S2B). Investigations of MICOS steady-state levels in these double deletion mutants strongly indicate a partial PaIAP-dependent regulation of the MICOS subunits (Figure 2C,E). In particular, in *ΔPaMic60* the other Mic60-subcomplex component PaMIC19 is not regulated by PaIAP, while the reduction of the core subunit PaMIC10 of the Mic10-subcomplex is partially PaIAP-dependent (Figure 2C,D). Analysis of Mic10-subcomplex mutants revealed that loss of components from both subcomplexes is at least partially PaIAP-dependent. In *ΔPaMic10* the protein abundance of PaMIC19 and
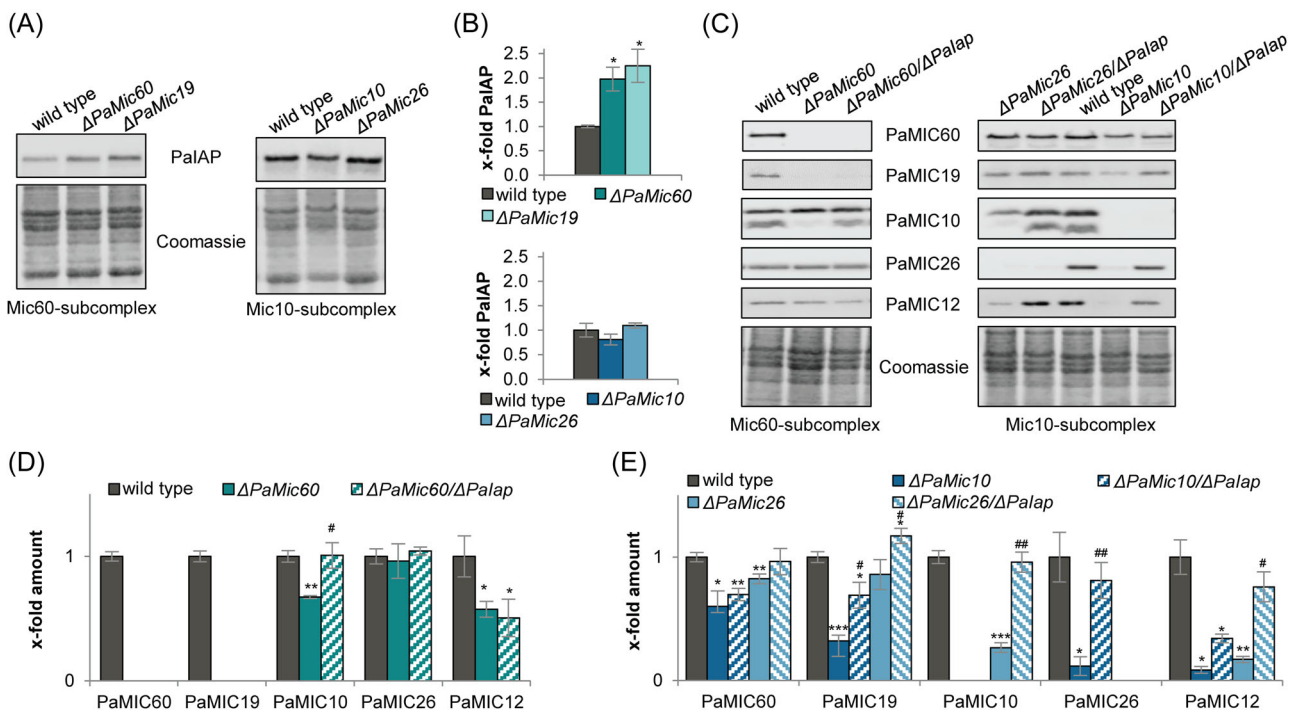
FIGURE 2 PaIAP-dependent regulation of MICOS steady-state levels. (A) Representative western blot analyses of mitochondrial protein extracts of *Podospora anserina* wild type, *ΔPaMic60, ΔPaMic19, ΔPaMic10*, and *ΔPaMic26* using a PaIAP antibody. (B) Quantification of PaIAP abundance normalized to the Coomassie-stained gel and related to the wild type (set to 1). Data are mean abundance ± SD (every three biological replicates). (C) Representative western blot analyses of mitochondrial protein extracts of *P. anserina* wild type, *ΔPaMic60* and *ΔPaMic60/ΔPaIap*, *ΔPaMic10* and *ΔPaMic10/ΔPaIap*, *ΔPaMic26* and *ΔPaMic26/ΔPaIap*. MICOS proteins were detected by specific antibodies. (D−E) Quantification of MICOS protein levels. MICOS protein levels were normalized to the Coomassie-stained gel and related to the wild type (set to 1). Data represent mean ± SD ($n = 3$). *Significant differences to wild type; #significant differences to the corresponding single MICOS deletion mutant. */#$p < 0.05$; **/##$p < 0.01$; ***/###$p < 0.001$. MICOS, mitochondrial contact site and cristae organizing system.

PaMIC26 is increased after simultaneous ablation of PaIAP indicating a regulation by the PaIAP protease (Figure 2C,E). Likewise, the abundance of PaMIC10, PaMIC12, and PaMIC19 in *ΔPaMic26* strains is PaIAP-dependent (Figure 2C,E). Our findings are in agreement with potential substrates of the iAAA protease from different organisms which were identified by substrate trapping assays. For instance, in *Arabidopsis thaliana* and *D. melanogaster* MIC60 was found as a potential substrate of the iAAA protease YME1.[62,63] Moreover, in yeast, MIC27, MIC10, MIC12, and MIC60 were identified as potential YME1 substrates.[64]

Taken together, our findings extend the current knowledge about the YME1/IAP-dependent regulation of the MICOS complex. Hitherto only a YME1-dependent regulation of MIC60 was known and now we demonstrated that the regulation of all MICOS subunits is partially mediated by the iAAA protease PaIAP. Such a proteolytic posttranslational regulation allows the organism to very quickly respond to environmental changes, like for example, different nutrient supply.

3.3 | Mitochondrial morphology and function are impaired by the ablation of MICOS subunits

Next, we set out to investigate whether impairments of MICOS have an impact on whole mitochondria. Since MICOS in yeast and humans is essential to maintain mitochondrial ultrastructure,[23,26,61] we compared mitochondrial cristae organization of MICOS deletion strains and wild-type strains by TEM (Figure 3A). Ablation of MICOS in *P. anserina* leads to characteristic alterations of the inner mitochondrial membrane morphology with stacks of cristae membranes and loss of crista junctions. As expected from earlier studies,[21,65] the wild type contains mostly filamentous mitochondria with short cristae, which are connected to the inner boundary membrane in 95% of the mitochondria (Figure 3A−C). In contrast, in *ΔPaMic60, ΔPaMic19, ΔPaMic10*, and *ΔPaMic26* mutants mitochondria are highly fragmented with cristae, which are not connected to the inner boundary membrane in 91%, 79%, 93%, and 89% of the mitochondria, respectively (Figure 3A−C). These floating cristae
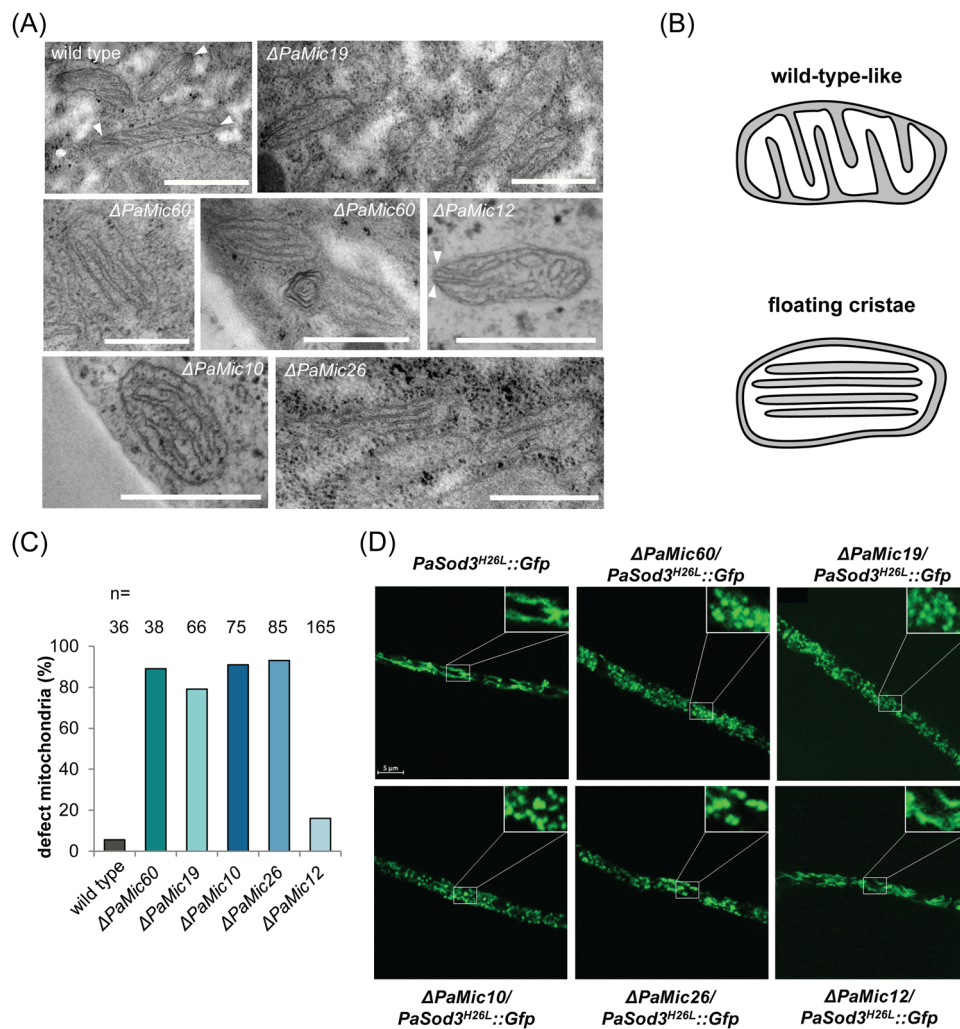
FIGURE 3 Ablation of MICOS subunits leads to mitochondrial alterations. (A) Representative TEM images of mitochondria from 50 nm thin sections of plastic embedded 6-day-old *Podospora anserina* mycelia of wild-type and MICOS deletion strains. Scale bar: 500 nm. White arrowheads point to cristae connected to the inner boundary membrane. (B) Scheme illustrates the two cristae structures. Above wild-type-like cristae with a connection to the inner boundary membrane and below floating cristae without any connection. (C) Quantification of the number of aberrant mitochondria with floating cristae in *P. anserina* wild type and MICOS mutants. n, number of mitochondria analyzed. (D) Fluorescence microscopic analysis of mitochondria from 6-day-old *P. anserina* wild-type and *ΔPaMic60*, *ΔPaMic19*, *ΔPaMic10*, *ΔPaMic26*, and *ΔPaMic12* strains with the mitochondrial reporter PaSOD3[H26L]::GFP. MICOS, mitochondrial contact site and cristae organizing system; TEM, transmission electron microscopy.

often form membrane stacks parallel to the longest mitochondrial axis. The only exception is the *ΔPaMic12* mutant, which mostly shows filamentous mitochondria with only a small fraction of about 16% of abnormal mitochondria. Similar, rather wild-type-like cristae structure was also described for yeast *Mic12* deletion strains.[23] In contrast, for ablation of the human MIC12 homolog MIC13 severe changes of the cristae such as in the other MICOS mutants were described.[61] The ultrastructural changes observed in *P. anserina* MICOS mutants (except for PaMIC12) are in concordance with findings from yeast and humans, which also describe characteristic cristae stacks.[23,26,31,61] Nevertheless, these ultrastructural changes in *P. anserina* MICOS mutants were clearly different from the known alterations of the ultrastructure in F_1F_o-ATP-synthase mutants or in senescent *P. anserina* wild-type strains. In the senescent *P. anserina* wild type the cristae formed a reticulate network resembling fishing nets.[11,65] A similar reticular or vesicular morphology of the cristae was also shown in *P. anserina* F_1F_o-ATP-synthase dimerization mutants.[21] These differences in cristae structures of MICOS and F_1F_o-ATP-synthase dimerization mutants were also described in yeast and explained by the different roles of these two complexes in cristae formation.[14] Accordingly, the MICOS complex is essential for the formation

of cristae junctions and the F_1F_o-ATP-synthase dimers are necessary for the formation of cristae tips. Hence, F_1F_o-ATP-synthase dimerization mutants cannot form cristae tips, leading to bridge-like cristae that extend across whole sections of mitochondria, ending on both sides with fused cristae junctions. Inner membranes forming vesicles in the old *P. anserina* wild type appear to result from the same mechanism as those resulting from the loss of F_1F_o-ATP-synthase dimers in strains lacking dimer assembly factors.[11,21] In contrast, in yeast MICOS mutants the F_1F_o-ATP-synthase dimers help shape the cristae tips but no cristae junctions can be formed to connect the cristae to the inner boundary membrane leading to floating cristae stacks.[14] A similar mechanism most likely also accounts for the floating cristae stacks in *P. anserina* MICOS mutants.

To assess whether these ultrastructural changes are accompanied by altered mitochondrial morphology, we performed fluorescence microscopy analysis. Therefore, we generated MICOS deletion strains expressing the gene coding for a specific mitochondrial marker protein, PaSOD3^H26L::GFP[42] (Supporting Information: Figure S2C,D). We found that, in contrast to the wild type, in which mitochondria are mainly filamentous, the MICOS mutants of both subcomplexes exhibit fragmented mitochondria (Figure 3D). In accordance with the data from the ultrastructure analysis, the *PaMic12* deletion strain is an exception and shows wild-type-like filamentous mitochondria. Our findings are in contrast to those from human cells, in which only the Mic60- but not the Mic10-subcomplex is crucial to maintain the mitochondrial network.[61] However, in MIC10-depleted yeast cells the mitochondrial network is frequently fragmented.[66]

Next, we investigated whether or not these morphological and ultrastructural changes in the MICOS mutants affect the composition of the respiratory chain. BN-PAGE analyses revealed that, compared to the wild type, the MICOS mutants of both subcomplexes showed only slight changes in the respiratory chain composition (Figure 4A). The amount of supercomplex S_0 and complex I are significantly reduced in Mic60-subcomplex mutants (Figure 4A,B). These complexes of the respiratory chain are also reduced in *PaMic10* and *PaMic26* deletion mutants (Figure 4A,B). All other complexes, such as F_1F_o-ATP-synthase dimers (V_2), are not altered compared to wild type. This is partially in contrast to what was found in other organisms. In human cell cultures, depending on which subunit of MICOS was deleted and which cell cultures were used, there are different findings reported. For instance, in HAP1 cells, double deletion of *Mic26* and *Mic27* led to drastic reduction of individual respiratory complexes and supercomplexes.[67] In contrast, in HeLa and HEK cells deletion of MICOS

subunits had only a modest impact on the composition of the respiratory chain.[31,68] Similar, in yeast only minor changes in respiratory chain composition were found.[31,66] As in our previous analyses, in the *PaMic12* deletion mutant no changes in the composition of the respiratory chain are present.

To experimentally investigate whether or not the changes in the respiratory chain composition affect the function of *P. anserina*, we measured the oxygen consumption rate (OCR) of isolated mitochondria by high-resolution respirometry. In accordance with the reduced complex I amount, we obtained a reduced complex I-dependent OCR in all MICOS mutants (Figure 4D,E). In particular, the state 4 OCR (ADP-limiting conditions) is reduced in mitochondria of *PaMic19* and *PaMic26* deletion strains compared to the wild type. The state 3 OCR (addition of ADP) is reduced in Mic60-subcomplex mutants of about 14% −21% and in Mic60-subcomplex mutants of about 22% −23%. These findings suggest an impaired mitochondrial function, which is more pronounced in the Mic10-subcomplex mutants. Similar respiratory impairments were also found in yeast and different cell lines.[31,61,67,68]

Taken together, the loss of MICOS leads to an altered ultrastructure and morphology of mitochondria and negatively affects the composition and function of the respiratory chain.

3.4 | Ablation of MICOS subunits leads to unexpected longevity of *P. anserina*

Next, we set out to investigate the consequences of the loss of MICOS for *P. anserina*. Phenotypic comparisons of strains revealed minor differences between the MICOS deletion mutants (except of *ΔPaMic12*) and the wild type (Figure 5A). Deletion mutants of the core subunits PaMIC60 and PaMIC10 show reduced rhythmic growth, exhibit a decreased pigmentation, and an increased formation of aerial hyphae. The deletion mutants of the regulatory subunits PaMIC19 and PaMIC26 show a similar but weaker phenotype. As in yeast,[23] the growth rates of all MICOS mutants are slightly reduced compared to the wild type (Figure 5B,E).

Although the impact of F_1F_o-ATP-synthase on mitochondrial ultrastructure and aging of *P. anserina* has been investigated experimentally, such an analysis was missing for MICOS until now. Fragmentation of mitochondrial network and loss of mitochondrial cristae structure are well-known as senescent markers in various organisms, including *P. anserina*.[11,65,69–75] Furthermore, we know that fragmentation of mitochondria, due to genetic manipulations or treatment with polyphenols, is
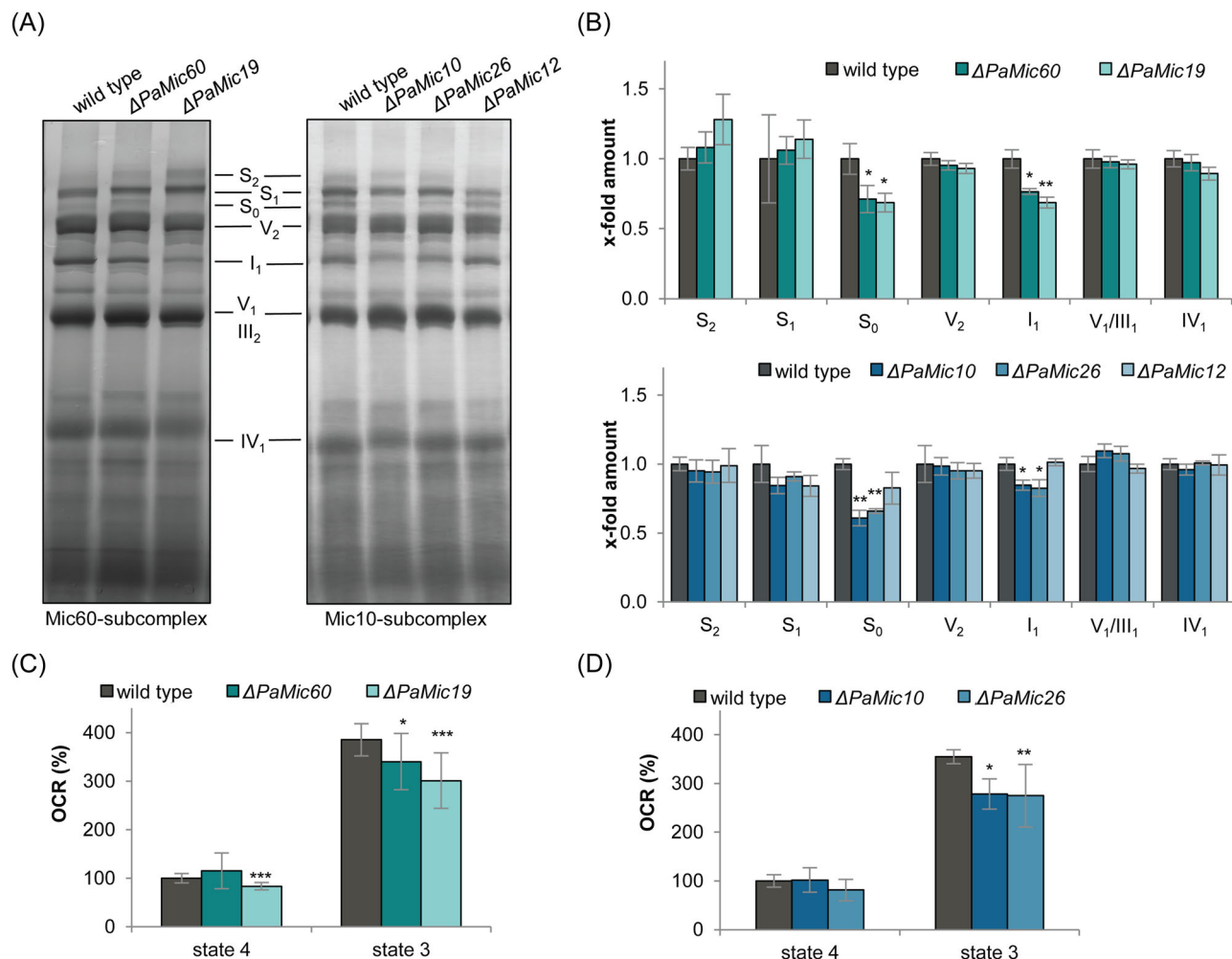
FIGURE 4 Ablation of MICOS subunits leads to mitochondrial impairments. (A) Representative BN-PAGE analysis and (B) quantification of isolated mitochondria from *Podospora anserina* wild-type and *ΔPaMic60*, *ΔPaMic19*, *ΔPaMic10*, *ΔPaMic26*, and *ΔPaMic12* cultures (three biological replicates for each culture). The supercomplexes (S_{0-2}; $I_1III_2IV_{0-2}$), dimeric complexes III and V (III_2 and V_2) as well as monomeric complexes I_1, IV_1, and V_1 were visualized by Coomassie staining. (C) Complex I-dependent oxygen consumption rate (OCR) of isolated mitochondria from wild-type, *ΔPaMic60* and *ΔPaMic19* cultures ($n = 3$ biological replicates, each with three to five technical replicates). State 4 OCR of wild-type mitochondria is set to 100%. (D) Complex I-dependent OCR of isolated mitochondria from wild-type, *ΔPaMic10* and *ΔPaMic26* cultures ($n = 2$ biological replicates, each with three to four technical replicates). State 4 OCR of wild-type mitochondria is set to 100%. Data represent mean $\pm$ SD. $*p < 0.05$; $**p < 0.01$; $***p < 0.01$; $**p < 0.01$. MICOS, mitochondrial contact site and cristae organizing system.

accompanied by lifespan reduction in *P. anserina*.[21,76] Very recently, a study aiming to develop a new high-throughput replicative lifespan screening with the yeast knockout collection uncovered as a side-effect a decreased replicative lifespan of a *Mic60* deletion strain.[77] This was the first hint for a possible impact of MICOS on aging. Nevertheless, a detailed analysis of this impact and of the possible basic mechanism is still missing. In our study, we analyzed the lifespan of all five *P. anserina* MICOS mutants under standard growth conditions and anticipated finding a lifespan reduction. Most surprisingly, the ablation of MICOS subunits led to a pronounced lifespan extension (Figure 5C,F; Supporting Information: Table S5). The mean lifespan of MICOS mutants is doubled compared to that of wild type (Figure 5D,G). In more detail, ablation of PaMIC60 and PaMIC19 leads to a mean lifespan increase of 88% (47 vs. 25 day) and 100% (50 vs. 25 day) and a maximal lifespan extension of 230% (105 vs. 32 day) and 180% (90 vs. 32 day), respectively (Figure 5C,F; Supporting Information: Table S5). Similarly, ablation of PaMIC10 and PaMIC26 leads to a mean lifespan increase of 56% (39 vs. 25 day) and 108% (52 vs. 25 day) and a maximal lifespan extension of 134% (75 vs. 32 day) and 213% (100 vs. 32 day), respectively (Figure 5F; Supporting Information: Table S5).
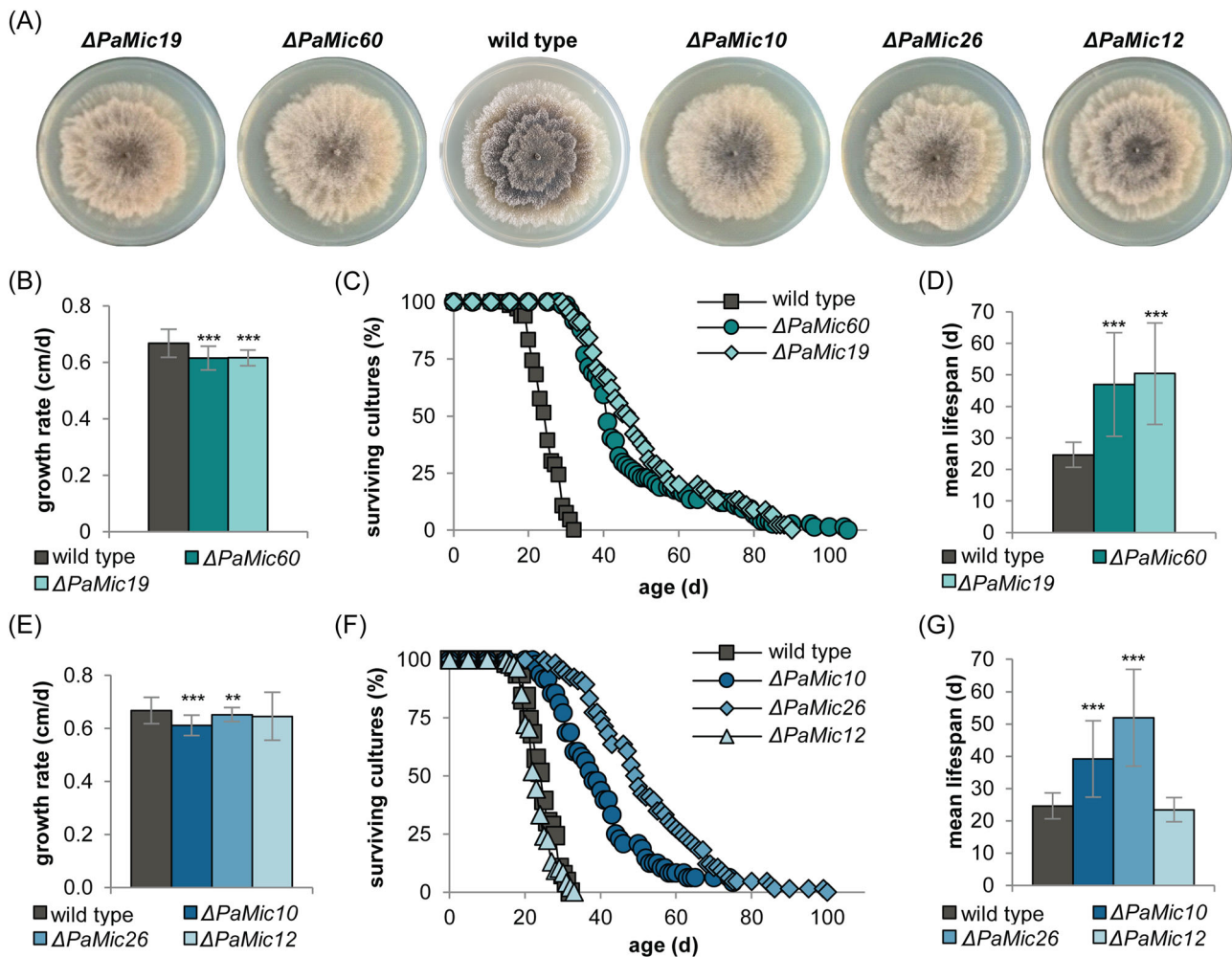
FIGURE 5 Ablation of MICOS leads to unexpected longevity. (A) Phenotype of 6-day-old *Podospora anserina* wild-type and *ΔPaMic60 ΔPaMic19*, *ΔPaMic10*, *ΔPaMic26*, and *ΔPaMic12* strains grown on standard BMM medium. (B) Growth rate and (C) survival curves of *P. anserina* wild type ($n = 66$); *ΔPaMic60* ($n = 74$), and *ΔPaMic19* ($n = 45$) grown on standard M2 medium. (D) Mean lifespan of cultures from (C). (E) Growth rate and (F) survival curves of *P. anserina* wild type ($n = 66$), *ΔPaMic10* ($n = 38$), *ΔPaMic26* ($n = 66$), and *ΔPaMic12* ($n = 54$) grown on standard M2 medium. (G) Mean lifespan of cultures from (F). Data represent mean ± SD. **$p < 0.01$; ***$p < 0.001$. MICOS, mitochondrial contact site and cristae organizing system. BMM, "Biomalz-Mais" Medium.

As the growth rate of the MICOS mutants is significantly reduced in comparison to the wild type it may be possible that the lifespan of the mutants measured in days is increased because of reduced metabolism and impairments in growth. We, therefore, measured the total growth distance of mutant colonies until they stopped growing and compared this distance to that of the wild type. Despite the reduction of the growth rate, the distance of growth of each of the analyzed MICOS mutants was strongly increased demonstrating that lifespan increase is not the result of slower growth (Supporting Information: Figure S3).

The lifespan extension of the *P. anserina* MICOS mutants is in contrast to the decreased replicative lifespan of the yeast *Mic60* deletion mutant,[77] which was identified as a side-effect in a high-throughput study

without in-depth characterization of the mutant. It is yet not clear, how robust this observation is. To learn whether or not the results obtained with *P. anserina* are conserved among species further studies with other organisms are required.

The observed lifespan extension of MICOS mutants is abrogated after the reintroduction of a wild-type copy of the corresponding genes in the MICOS deletion mutants (Supporting Information: Figure S4). Again, the *PaMic12* deletion mutant is an exception (Figure 5F). This, together with the observation that in *ΔPaMic12* neither ultrastructure nor the level of other MICOS components is affected, prompts us to speculate about the role of PaMIC12. It might be possible that PaMIC12 is not a central component of the *P. anserina* MICOS. However, the fact that the loss of all other MICOS subunits has an

impact on the PaMIC12 steady-state level argues against this possibility (Figure 1B,C). In yeast, MIC12 was shown to function as a coupling factor promoting the interaction of the two MICOS subcomplexes.[78] The weak phenotype of *ΔPaMic12* can also be explained by the independent roles of the two MICOS subcomplexes, which are not affected upon loss of the coupling factor (Figure 1B,C).

The longevity of MICOS mutants is a counterintuitive finding, since manipulation of the two other cristae-shaping components, F_1F_o-ATP-synthase, and cardiolipin, has negative effects on organismic aging in *P. anserina* leading to lifespan reduction.[28,40] Therefore, we asked how these opposing effects on the lifespan could occur. What might be the physiological reason or the advantages of these differences? Although future experiments will have to provide the answers to these questions, from our results and the literature, we propose that the reason is the biogenesis of cristae and in the physiological effects of the changes. Various studies demonstrated different ways of cristae formation with different roles of the MICOS complex and the F_1F_o-ATP-synthase dimers.[12,61] Recently, it was postulated that cristae and cristae junctions are highly dynamic undergoing continuous fusion and fission processes.[79] Further, it was shown that re-expression of MICOS proteins in MICOS deletion cell lines could induce secondary cristae junction formation.[61] In these studies, the authors assume that cristae stacks in MICOS mutants represent an intermediate structure that also occurs during normal cristae formation in the wild type.[61] Hence, we propose that floating cristae in the *P. anserina* MICOS mutants are in some way advantageous compared to the vesicles formed in the F_1F_o-ATP-synthase dimerization mutants. Besides the different cristae structures, probably the most important difference is the presence of F_1F_o-ATP-synthase dimers in the MICOS mutants which are missing in F_1F_o-ATP-synthase dimerization mutants. This difference may lead to different physiological effects in the different mutants.

3.5 | Loss of MICOS leads to increased reactive oxygen species (ROS) levels and induction of mitophagy

Next, we set out to investigate physiological effects explaining the mechanistic basis of the unexpected lifespan increase of the MICOS mutants. A previous study revealed that mitophagy can act as a pro-survival mechanism in a mitochondrial quality control mutant of *P. anserina*.[42] To analyze mitophagy in MICOS mutants we performed a biochemical analysis using a vacuolar GFP-cleavage assay.[80,81] In this assay the vacuolar

degradation of the mitochondrial PaSOD3[H26L]::GFP fusion reporter protein is monitored. When PaSOD3[H26L]::GFP labeled mitochondria have entered the vacuole a degradation-resistant GFP-part ("free GFP"), which was liberated from the fusion protein through proteolytic digestion, can be detected in western blots indicating ongoing mitophagy.[42] Western blot analysis revealed a nearly 1.5-fold increase in the amount of "free GFP" in the Mic60-subcomplex mutants *ΔPaMic60* and *ΔPaMic19* (Figure 6A,B). Similarly, in Mic10-subcomplex mutants, we also observed a "free GFP" increase. In *ΔPaMic10* as well as *ΔPaMic26* the amount of "free GFP" significantly increases 1.5-fold compared to the wild type (Figure 6C,D), indicating an upregulation of the mitophagy rate. In accordance with these data, in human cell lines and in *D. melanogaster* it was recently shown that mitophagy was induced after ablation of MIC60.[82,83] As expected, in the *PaMic12* deletion mutant no increase of "free GFP" was detected (Supporting Information: Figure S5). The rather slight increase of mitophagy in MICOS mutants is a marked difference from the strong increase of mitophagy (sixfold increase) in F_1F_o-ATP-synthase dimerization mutants.[22]

The induction of mitophagy can have different causes. One of the most commonly described causes is the induction of oxidative stress due to increased levels of ROS.[84,85] Accordingly, in HeLa cells missing MIC60 increased ROS production was found.[86] To test whether or not ROS levels are altered in the *P. anserina* MICOS mutants, we used a histochemically method to visualize the extracellular amount of the two common ROS, superoxide anion and hydrogen peroxide.[87] This is an indirect measure of ROS levels in the different compartments of the cell. In contrast to the F_1F_o-ATP-synthase dimerization mutants,[22] we observed no changes in the hydrogen peroxide levels, but an increase in superoxide anion level in the MICOS mutants compared to the wild type (Figure 6E,F). The latter is indicated by the accumulation of a lilac precipitate specifically at the growth front of the mycelium. These data suggest that superoxide formation is the trigger for the mild mitophagy induction in MICOS mutants.

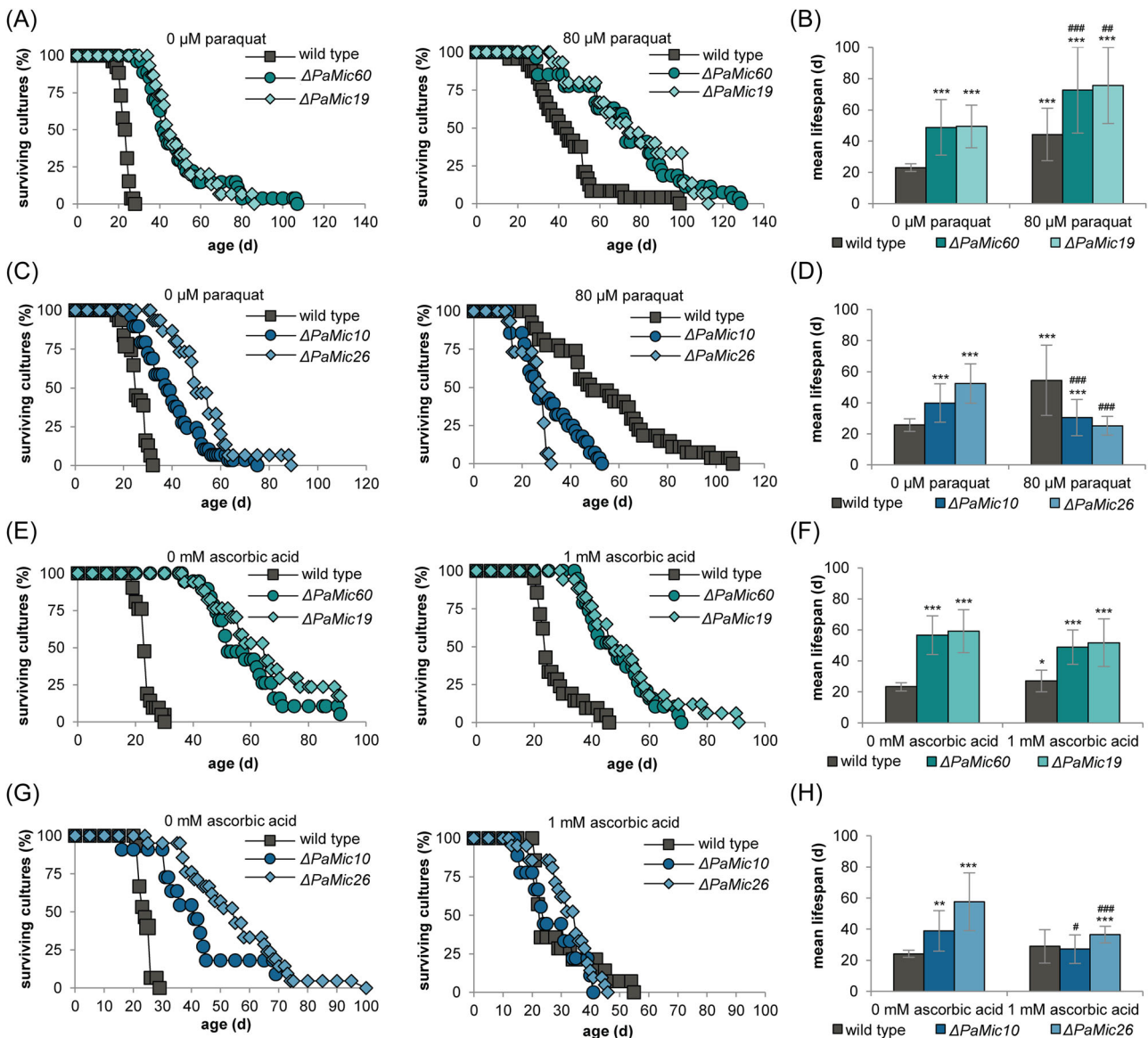## 3.6 | Lifespan extension of Mic10-subcomplex mutants is ROS-dependent

In biological systems, such as *Caenorhabditis elegans*, mild oxidative stress, due to elevated superoxide anion levels, is known to cause longevity. This beneficial effect of mild oxidative stress is termed mitohormesis.[88,89] A similar lifespan extending adaptive response was described upon RNAi-mediated or frataxin-mediated mitochondrial
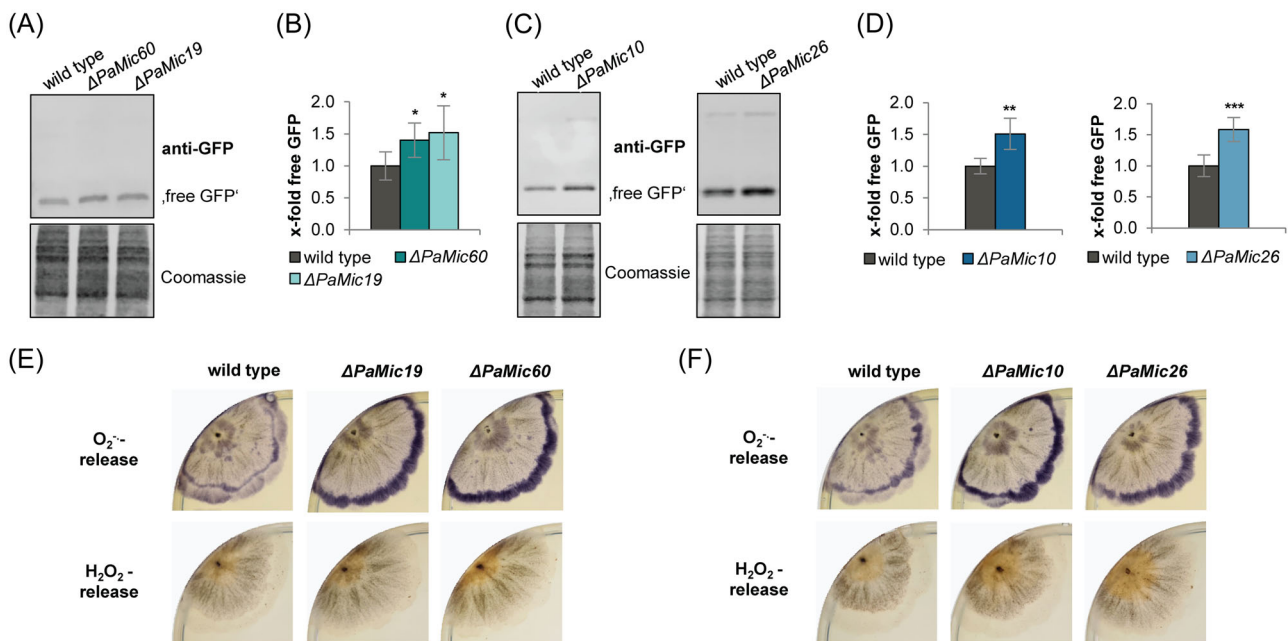
FIGURE 6 Disruption of MICOS leads to mitophagy induction and oxidative stress. (A) Monitoring mitophagy by western blot analysis of total protein extracts from $PaSod3^{H26L}::Gfp$ (here wild type), $\Delta PaMic60/PaSod3^{H26L}::Gfp$ (here $\Delta PaMic60$), and $\Delta PaMic19/PaSod3^{H26L}::Gfp$ (here $\Delta PaMic19$) cultures with a GFP antibody (every six biological replicates). (B) Quantification of "free GFP" protein level from (A) normalized to the Coomassie-stained gel. Protein level in $PaSod3^{H26L}::Gfp$ cultures was set to 1. Data represent mean ± SD. (C) Monitoring mitophagy by western blot analysis of total protein extracts from $PaSod3^{H26L}::Gfp$ (here wild type), $\Delta PaMic10/PaSod3^{H26L}::Gfp$ (here $\Delta PaMic10$), and $\Delta PaMic26/PaSod3^{H26L}::Gfp$ (here $\Delta PaMic26$) cultures with a GFP antibody (each 5−7 biological replicates). (D) Quantification of "free GFP" protein level from (C) normalized to the Coomassie-stained gel. Protein level in $PaSod3^{H26L}::Gfp$ cultures was set to 1. (E, F) Qualitative determination of superoxide anion and hydrogen peroxide release by histochemical NBT- and DAB-staining of *Podospora anserina* wild type and $\Delta PaMic60$, $\Delta PaMic19$, $\Delta PaMic10$, and $\Delta PaMic26$ strains. *Significant differences to the wild type *$p < 0.05$; **$p < 0.01$; ***$p < 0.001$. DAB, diaminobenzidine; MICOS, mitochondrial contact site and cristae organizing system; NBT, nitro blue tetrazolium.

stress.[90–92] In *P. anserina* it was also previously shown that superoxide anion-triggered mitophagy participates in mitohormesis.[42] Hence, we hypothesized that the longevity of MICOS mutants is caused by mitohormesis. To experimentally validate this hypothesis, we analyzed the lifespan of the MICOS mutants and the wild type under oxidative stress induced by paraquat, a well-known herbicide that induces mitochondrial superoxide stress.[93] Normally, treatment with low paraquat concentrations (20−80 μM) results in a mitohormetic, pronounced lifespan extension, which is lost at higher paraquat concentrations.[42,94] However, if the observed lifespan extension of the MICOS mutants is due to a ROS-dependent mitohormetic response, additional mild paraquat treatment should pass beneficial ROS levels and lead to a reduced lifespan. Consistent with previously published data[42] we found that mild paraquat-induced oxidative stress has a lifespan-prolonging effect in the *P. anserina* wild type (Figure 7A,B; Suppporting Information: Table S6). The treatment with 80 μM paraquat prolongs the mean lifespan of the wild type by about 87% (43 vs. 23 day). Likewise, the lifespans of the $\Delta PaMic60$ and $\Delta PaMic19$ mutants are further increased

by 80 μM paraquat compared to the untreated mutant (Figure 7A). The mean lifespans of the paraquat-treated $\Delta PaMic60$ and $\Delta PaMic19$ mutant are extended by at least 45% (68 vs. 47 day) and 52% (76 vs. 50 day), respectively (Figure 7B; Suppporting Information: Table S6). In contrast, the lifespans of the $\Delta PaMic10$ and $\Delta PaMic26$ mutants are decreased by treatment with 80 μM paraquat (Figure 7C,D; Suppporting Information: Table S7). The mean lifespans of the $\Delta PaMic10$ and $\Delta PaMic26$ mutants are reduced by at least 18% (32 vs. 39 day) and 45% (29 vs. 52 day), respectively (Figure 7D; Suppporting Information: Table S7). Thus, obviously, 80 μM paraquat overwhelms the repair and recycling capacity of Mic10-subcomplex mutants, while Mic60-subcomplex mutants still have enough capacity. A mitohormetic response requires efficient transmission of the stress signal from the mitochondria to the cytosol and the nucleus. We speculate that this retrograde signaling is impaired upon ablation of Mic60-subcomplex due to its role in forming the contact between the inner and outer mitochondrial membrane. Thus, although the appropriate signal (increased superoxide level) is present, the outcome is not identical in

FIGURE 7 Lifespan extension of Mic10-subcomplex mutants is ROS-dependent. (A) Survival curves of *Podospora anserina* wild type ($n = 26$), *ΔPaMic60* ($n = 27$), and *ΔPaMic19* ($n = 15$) grown on standard M2 medium with or without 80 µM paraquat. (B) Mean lifespan of cultures from (A). (C) Survival curves of *P. anserina* wild type ($n = 27$), *ΔPaMic10* ($n = 28$), and *ΔPaMic26* ($n = 27$) grown on standard M2 medium with or without 80 µM paraquat. (D) Mean lifespan of cultures from (C). (E) Survival curves of *P. anserina* wild type ($n = 21$), *ΔPaMic60* ($n = 19$), and *ΔPaMic19* ($n = 17$) grown on standard M2 medium with or without 1 mM ascorbic acid. (F) Mean lifespan of cultures from (E). (G) Survival curves of *P. anserina* wild type ($n = 15$), *ΔPaMic10* ($n = 11$), and *ΔPaMic26* ($n = 20$) grown on standard M2 medium with or without 1 mM ascorbic acid. (H) Mean lifespan of cultures from (G). Data represent mean ± SD. *Significant differences to the wild type without paraquat/ascorbic acid; #significant differences to the corresponding deletion mutant without paraquat/ascorbic acid. **/##$p < 0.01$; ***/###$p < 0.001$.

Mic10- and Mic60-subcomplex mutants. In Mic10-subcomplex mutants a strong mitohormetic response is induced in Mic10-subcomplex mutants, which is hardly effective in Mic60-subcomplex mutants. Additional ROS stress (80 µM paraquat) becomes detrimental in Mic10-subcomplex mutants leading to lifespan reduction. In contrast, in the Mic60-subcomplex mutants, additional ROS stress (80 µM) is required to enhance the retrograde

signal to stimulate a beneficial mitohormetic response. This conclusion suggests that in Mic60-subcomplex mutants another pathway leads to longevity, while longevity in the Mic10-subcomplex mutants seems to be completely ROS-dependent.

To verify this assumption, we analyzed the lifespan of the MICOS mutants under ROS scavenging conditions. Thereby the enhanced superoxide anions are scavenged
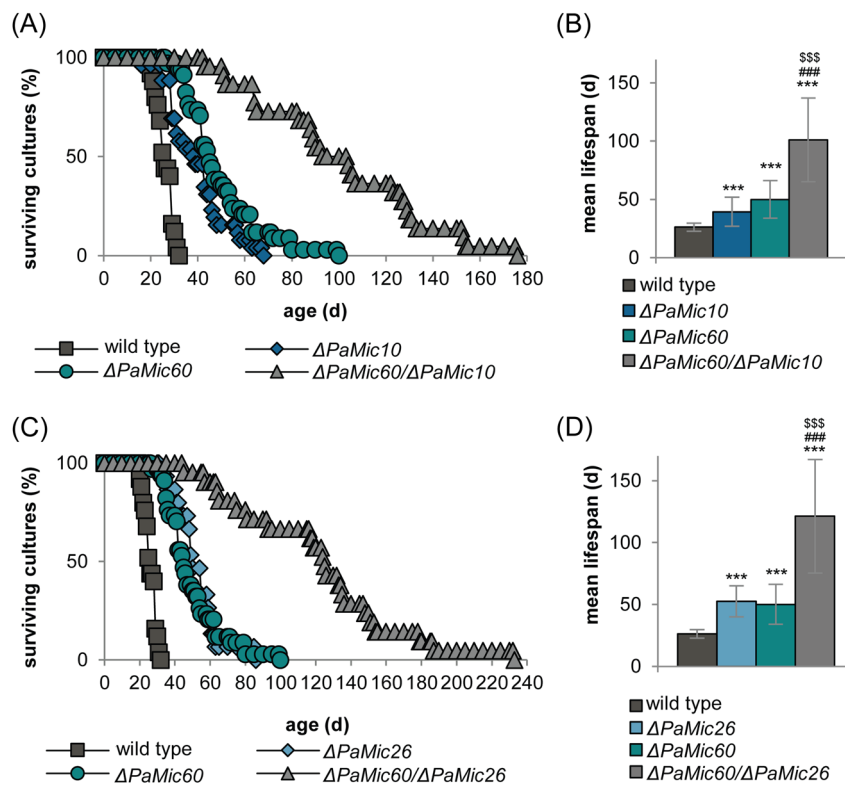
FIGURE 8 Simultaneous ablation of subunits from both MICOS subcomplex synergistically increases lifespan. (A) Survival curves of *Podospora anserina* wild type ($n = 25$), *ΔPaMic60* ($n = 34$), *ΔPaMic10* ($n = 27$), and *ΔPaMic60/ΔPaMic10* ($n = 22$) grown on standard M2 medium. (B) Mean lifespan of cultures from (A). (C) Survival curves of *P. anserina* wild type ($n = 25$), *ΔPaMic60* ($n = 34$), *ΔPaMic26* ($n = 15$), and *ΔPaMic60/ΔPaMic26* ($n = 23$) grown on standard M2 medium. (D) Mean lifespan of cultures from (C). Data represent mean ± SD. ***Significant differences to wild type; \#\#\#significant differences to *ΔPaMic26* or *ΔPaMic10*; $$$significant differences to *ΔPaMic60*. $p < 0.001$. MICOS, mitochondrial contact site and cristae organizing system.

by the antioxidant ascorbic acid. As assumed, under these conditions we obtained only slight differences in the *ΔPaMic60* and *ΔPaMic19* lifespan (Figure 7E,F; Suppporting Information: Table S6). The mean lifespan of the *ΔPaMic60* mutant is slightly reduced by 10% (49 vs. 54 day) compared to the untreated mutant (Figure 7F; Suppporting Information: Table S7). Comparably, the mean lifespan of the *ΔPaMic19* mutant is reduced by 14% (49 vs. 57 day). In contrast, ROS scavenging in *ΔPaMic10* and *ΔPaMic26* (Figure 7G,H; Suppporting Information: Table S7) led to a strong lifespan reduction. The mean lifespan of the *ΔPaMic26* mutant is reduced by more than 36% (37 vs. 58 day) compared to the untreated mutant (Figure 7G; Suppporting Information: Table S7). Comparably, the mean lifespan of the *ΔPaMic10* mutant is reduced by more than 35% (27 vs. 36 day). These data verify that longevity of Mic10-subcomplex mutants depends on ROS-induced mitohormesis.

Retrograde signals from mitochondria upon oxidative stress and damage can be very diverse. For instance, peptides from the proteolytic degradation of damaged or misfolded proteins, a reduced mitochondrial membrane potential or lipid peroxidation, and a consequently altered lipid composition of the outer mitochondrial membrane can activate signal cascades. Moreover, congestion of protein transport into mitochondria can act as a stress signal.[95–98] As mentioned above, we suggest that retrograde signaling is impaired in Mic60-subcomplex mutants because of the compromised contact between the inner and outer mitochondrial membrane. This hypothesis is confirmed by the observation that mitochondrial import defects are consequences of MICOS disruption in yeast.[27,99] For an efficient protein import, an interaction between the Mic60-subcomplex and the protein import machinery is necessary.[23,26,100]

3.7 | Both MICOS subcomplexes act in parallel pathways to regulate lifespan

If the mitohormetic response is attenuated in the Mic60-subcomplex mutants and in Mic10-subcomplexes this response is active leading to lifespan extension, a double mutant lacking both subcomplexes should show an

additive effect and further lifespan extension. To test this possibility, we generated double mutants in which one subunit of each subcomplex is missing (Suppporting Information: Figure S6). And indeed, a double mutant missing both core subunits shows a spectacular lifespan extension compared to the single mutants (Figure 8A,B). The mean lifespan of the *ΔPaMic60/ΔPaMic10* mutant is increased by 100% and 159%, respectively, compared to the single *ΔPaMic60* and *ΔPaMic10* mutants (Figure 8B; Suppporting Information: Table S8). Likewise, the simultaneous deletion of *PaMic60* and *PaMic26* was also found to be synergistically leading to a mean lifespan extension of more than 121 days (Figure 8C,D; Suppporting Information: Table S8). This is an increase of 142% and 133%, respectively, compared to the *ΔPaMic60* and *ΔPaMic26* single mutants. The lifespan analyses of the double mutants revealed that the longevity of Mic60-subcomplex mutants is based on a pathway that is distinct from that of the Mic10-subcomplex mutants.

Previous studies point out a connection between the MICOS complex and mitochondrial phospholipids. In yeast, the MICOS complex is necessary for phospholipid transfer between the inner and outer mitochondrial membrane.[101] Moreover, in human cells proteins of the phospholipid metabolism, for example, the CRD1, interact in a large protein complex with mitochondrial membrane proteins like MIC60 and MIC19.[102] In two recent studies, we found that in *P. anserina* mitochondrial phospholipid homeostasis affects the aging process,[51] that the abundance of cardiolipin synthase PaCRD1 is increased in Mic60-subcomplex mutants, and that mitochondrial phospholipid composition is altered indicating an impact of phospholipid homeostasis on lifespan control of Mic60-subcomplex mutants.[103]

4 | CONCLUSIONS

In the current study, we uncovered a counterintuitive and unexpected biological role of MICOS. Ablation of MICOS components in *P. anserina* leads to changes in mitochondrial cristae ultrastructure and morphology and to a pronounced lifespan extension. By the use of double mutants lacking both subcomplexes, we provide the first genetic evidence that the two MICOS subcomplexes impact organismic aging via different pathways. Although the longevity of Mic10-subcomplex mutants is triggered by ROS-induced mitohormesis, the pathway leading to the longevity of the Mic60-subcomplex mutants is linked to phospholipid homeostasis. This distinction may be due to the role of MIC60 in forming the contact between the outer and inner mitochondrial membrane as well as in mitochondrial protein import. Future studies need to address the question of whether this longevity pathway in MICOS mutants is evolutionary conserved from simple organisms like *P. anserina* up to humans.

AUTHOR CONTRIBUTIONS

Verena Warnsmann and Heinz D. Osiewacz designed this study and wrote the manuscript. Verena Warnsmann, Lisa-Marie Marschall, Anja C. Meeßen, Maike Wolters, Lea Schürmanns, Marion Basoglu, and Stefan Eimer performed experiments. Verena Warnsmann, Lisa-Marie Marschall, Stefan Eimer, and Heinz D. Osiewacz analyzed data. Verena Warnsmann visualized data. Heinz D. Osiewacz, Stefan Eimer, and Verena Warnsmann reviewed and edited the manuscript. Heinz D. Osiewacz supervised the study and acquired funding. All authors have read the final version of the manuscript.

CONFLICT OF INTEREST

The authors declare no conflict of interest.

DATA AVAILABILITY STATEMENT

The data that support the findings of this study are available on request from the corresponding author.

ORCID

Verena Warnsmann https://orcid.org/0000-0001-7358-4180
Heinz D. Osiewacz http://orcid.org/0000-0002-0360-6994

REFERENCES

1. Breitenbach M, Laun P, Dickinson JR, et al. The role of mitochondria in the aging processes of yeast. *Subcell Biochem*. 2012;57:55-78. doi:10.1007/978-94-007-2561-4_3
2. Kauppila TES, Kauppila JHK, Larsson NG. Mammalian mitochondria and aging: an update. *Cell Metab*. 2017;25(1):57-71. doi:10.1016/j.cmet.2016.09.017
3. Osiewacz HD. Role of mitochondria in aging and age-related disease. *Exp Gerontol*. 2010;45(7-8):465. doi:10.1016/j.exger.2010.05.001
4. Sun N, Youle RJ, Finkel T. The mitochondrial basis of aging. *Mol Cell*. 2016;61(5):654-666. doi:10.1016/j.molcel.2016.01.028
5. Tatsuta T, Langer T. Quality control of mitochondria: protection against neurodegeneration and ageing. *EMBO J*. 2008;27(2):306-314. doi:10.1038/sj.emboj.7601972

6. Frey TG, Mannella CA. The internal structure of mitochondria. *Trends Biochem Sci.* 2000;25(7):319-324. doi:10.1016/s0968-0004(00)01609-1

7. Klecker T, Westermann B. Pathways shaping the mitochondrial inner membrane. *Open Biol.* 2021;11(12):210238. doi:10.1098/rsob.210238

8. Zick M, Rabl R, Reichert AS. Cristae formation-linking ultrastructure and function of mitochondria. *Biochim Biophys Acta.* 2009;1793(1):5-19. doi:10.1016/j.bbamcr.2008.06.013

9. Mannella CA. The relevance of mitochondrial membrane topology to mitochondrial function. *Biochim Biophys Acta.* 2006;1762(2):140-147. doi:10.1016/j.bbadis.2005.07.001

10. Colina-Tenorio L, Horten P, Pfanner N, Rampelt H. Shaping the mitochondrial inner membrane in health and disease. *J Intern Med.* 2020;287(6):645-664. doi:10.1111/joim.13031

11. Daum B, Walter A, Horst A, Osiewacz HD, Kühlbrandt W. Age-dependent dissociation of ATP synthase dimers and loss of inner-membrane cristae in mitochondria. *Proc Natl Acad Sci USA.* 2013;110(38):15301-15306. doi:10.1073/pnas.1305462110

12. Harner ME, Unger AK, Geerts WJ, et al. An evidence based hypothesis on the existence of two pathways of mitochondrial crista formation. *eLife.* 2016;5:e18853. doi:10.7554/eLife.18853

13. Martensson CU, Doan KN, Becker T. Effects of lipids on mitochondrial functions. *Biochim Biophys Acta Mol Cell Biol Lipids.* 2017;1862(1):102-113. doi:10.1016/j.bbalip.2016.06.015

14. Rabl R, Soubannier V, Scholz R, et al. Formation of cristae and crista junctions in mitochondria depends on antagonism between Fcj1 and Su e/g. *J Cell Biol.* 2009;185(6):1047-1063. doi:10.1083/jcb.200811099

15. Bornhövd C, Vogel F, Neupert W, Reichert AS. Mitochondrial membrane potential is dependent on the oligomeric state of F_1F_0-ATP synthase supracomplexes. *J Biol Chem.* 2006;281(20):13990-13998. doi:10.1074/jbc.M512334200

16. Davies KM, Anselmi C, Wittig I, Faraldo-Gomez JD, Kühlbrandt W. Structure of the yeast F_1F_o-ATP synthase dimer and its role in shaping the mitochondrial cristae. *Proc Natl Acad Sci USA.* 2012;109(34):13602-13607. doi:10.1073/pnas.1204593109

17. Strauss M, Hofhaus G, Schröder RR, Kühlbrandt W. Dimer ribbons of ATP synthase shape the inner mitochondrial membrane. *EMBO J.* 2008;27(7):1154-1160. doi:10.1038/emboj.2008.35

18. Arnold I, Pfeiffer K, Neupert W, Stuart RA, Schägger H. Yeast mitochondrial F_1F_0-ATP synthase exists as a dimer: identification of three dimer-specific subunits. *EMBO J.* 1998;17(24):7170-7178. doi:10.1093/emboj/17.24.7170

19. Habersetzer J, Larrieu I, Priault M, et al. Human F_1F_0 ATP synthase, mitochondrial ultrastructure and OXPHOS impairment: a (super-)complex matter? *PLoS One.* 2013;8(10):e75429. doi:10.1371/journal.pone.0075429

20. Paumard P, Vaillier J, Coulary B, et al. The ATP synthase is involved in generating mitochondrial cristae morphology. *EMBO J.* 2002;21(3):221-230. doi:10.1093/emboj/21.3.221

21. Rampello NG, Stenger M, Westermann B, Osiewacz HD. Impact of F_1F_o-ATP-synthase dimer assembly factors on mitochondrial function and organismic aging. *Microb Cell.* 2018;5:198-207. doi:10.15698/mic2018.04.625

22. Warnsmann V, Marschall L-M, Osiewacz HD. Impaired F_1F_o-ATP-synthase dimerization leads to the induction of cyclophilin D-mediated autophagy-dependent cell death and accelerated aging. *Cells.* 2021;10(4):757.

23. Harner M, Körner C, Walther D, et al. The mitochondrial contact site complex, a determinant of mitochondrial architecture. *EMBO J.* 2011;30(21):4356-4370. doi:10.1038/emboj.2011.379

24. Hoppins S, Collins SR, Cassidy-Stone A, et al. A mitochondrial-focused genetic interaction map reveals a scaffold-like complex required for inner membrane organization in mitochondria. *J Cell Biol.* 2011;195(2):323-340. doi:10.1083/jcb.201107053

25. van der Laan M, Bohnert M, Wiedemann N, Pfanner N. Role of MINOS in mitochondrial membrane architecture and biogenesis. *Trends Cell Biol.* 2012;22(4):185-192. doi:10.1016/j.tcb.2012.01.004

26. von der Malsburg K, Müller JM, Bohnert M, et al. Dual role of mitofilin in mitochondrial membrane organization and protein biogenesis. *Dev Cell.* 2011;21(4):694-707. doi:10.1016/j.devcel.2011.08.026

27. Khosravi S, Harner ME. The MICOS complex, a structural element of mitochondria with versatile functions. *Biol Chem.* 2020;401(6-7):765-778. doi:10.1515/hsz-2020-0103

28. Rampelt H, Zerbes RM, van der Laan M, Pfanner N. Role of the mitochondrial contact site and cristae organizing system in membrane architecture and dynamics. *Biochim Biophys Acta, Mol Cell Res.* 2017;1864(4):737-746. doi:10.1016/j.bbamcr.2016.05.020

29. Wollweber F, von der Malsburg K, van der Laan M. Mitochondrial contact site and cristae organizing system: a central player in membrane shaping and crosstalk. *Biochim Biophys Acta, Mol Cell Res.* 2017;1864(9):1481-1489. doi:10.1016/j.bbamcr.2017.05.004

30. Acehan D, Malhotra A, Xu Y, Ren M, Stokes DL, Schlame M. Cardiolipin affects the supramolecular organization of ATP synthase in mitochondria. *Biophys J.* 2011;100(9):2184-2192. doi:10.1016/j.bpj.2011.03.031

31. Friedman JR, Mourier A, Yamada J, McCaffery JM, Nunnari J. MICOS coordinates with respiratory complexes and lipids to establish mitochondrial inner membrane architecture. *eLife.* 2015;4:e07739. doi:10.7554/eLife.07739

32. Beltran-Heredia E, Tsai FC, Salinas-Almaguer S, Cao FJ, Bassereau P, Monroy F. Membrane curvature induces cardiolipin sorting. *Commun Biol.* 2019;2(225):225. doi:10.1038/s42003-019-0471-x

33. Khalifat N, Puff N, Bonneau S, Fournier JB, Angelova MI. Membrane deformation under local pH gradient: mimicking mitochondrial cristae dynamics. *Biophys J.* 2008;95(10):4924-4933. doi:10.1529/biophysj.108.136077

34. Acehan D, Xu Y, Stokes DL, Schlame M. Comparison of lymphoblast mitochondria from normal subjects and patients with Barth syndrome using electron microscopic tomography. *Lab Invest.* 2007;87(1):40-48. doi:10.1038/labinvest.3700480

35. Baile MG, Sathappa M, Lu YW, et al. Unremodeled and remodeled cardiolipin are functionally indistinguishable in yeast. *J Biol Chem.* 2014;289(3):1768-1778. doi:10.1074/jbc.M113.525733

36. Claypool SM, Boontheung P, McCaffery JM, Loo JA, Koehler CM. The cardiolipin transacylase, tafazzin, associates with two distinct respiratory components providing insight into Barth syndrome. *Mol Biol Cell.* 2008;19(12): 5143-5155. doi:10.1091/mbc.E08-09-0896

37. Pan R, Jones AD, Hu J. Cardiolipin-mediated mitochondrial dynamics and stress response in *Arabidopsis. Plant Cell.* 2014;26(1):391-409. doi:10.1105/tpc.113.121095

38. Pineau B, Bourge M, Marion J, et al. The importance of cardiolipin synthase for mitochondrial ultrastructure, respiratory function, plant development, and stress responses in *Arabidopsis. Plant Cell.* 2013;25(10):4195-4208. doi:10.1105/tpc.113.118018

39. Xu Y, Condell M, Plesken H, et al. A *Drosophila* model of Barth syndrome. *Proc Natl Acad Sci USA.* 2006;103(31): 11584-11588. doi:10.1073/pnas.0603242103

40. Löser T, Joppe A, Hamann A, Osiewacz HD. Mitochondrial phospholipid homeostasis is regulated by the i-AAA protease PaIAP and affects organismic aging. *Cells.* 2021;10(10):2775. doi:10.3390/cells10102775

41. Rizet G. Impossibility of obtaining uninterrupted and unlimited multiplication of the ascomycete *Podospora anserina. C R Hebd Seances Acad Sci.* 1953;237(15):838-840.

42. Knuppertz L, Warnsmann V, Hamann A, Grimm C, Osiewacz HD. Stress-dependent opposing roles for mitophagy in aging of the ascomycete *Podospora anserina. Autophagy.* 2017;13(6):1037-1052. doi:10.1080/15548627.2017.1303021

43. Weil A, Luce K, Dröse S, Wittig I, Brandt U, Osiewacz HD. Unmasking a temperature-dependent effect of the *P. anserina* i-AAA protease on aging and development. *Cell Cycle.* 2011;10(24):4280-4290. doi:10.4161/cc.10.24.18560

44. Osiewacz HD, Hamann A, Zintel S. Assessing organismal aging in the filamentous fungus *Podospora anserina. Methods Mol Biol.* 2013;965:439-462. doi:10.1007/978-1-62703-239-1_29

45. El-Khoury R, Sellem CH, Coppin E, et al. Gene deletion and allelic replacement in the filamentous fungus *Podospora anserina. Curr Genet.* 2008;53(4):249-258. doi:10.1007/s00294-008-0180-3

46. Kunstmann B, Osiewacz HD. The *S*-adenosylmethionine dependent *O*-methyltransferase PaMTH1: a longevity assurance factor protecting *Podospora anserina* against oxidative stress. *Aging (Albany NY).* 2009;1(3):328-334. doi:10.18632/aging.100029

47. Knuppertz L, Hamann A, Pampaloni F, Stelzer E, Osiewacz HD. Identification of autophagy as a longevity-assurance mechanism in the aging model *Podospora anserina. Autophagy.* 2014;10(5):822-834. doi:10.4161/auto.28148

48. Lecellier G, Silar P. Rapid methods for nucleic acids extraction from Petri dish-grown mycelia. *Curr Genet.* 1994;25(2):122-123. doi:10.1007/BF00309536

49. Luce K, Osiewacz HD. Increasing organismal healthspan by enhancing mitochondrial protein quality control. *Nat Cell Biol.* 2009;11(7):852-858. doi:10.1038/ncb1893

50. Zintel S, Schwitalla D, Luce K, Hamann A, Osiewacz HD. Increasing mitochondrial superoxide dismutase abundance leads to impairments in protein quality control and ROS scavenging systems and to lifespan shortening. *Exp Gerontol.* 2010;45(7-8):525-532. doi:10.1016/j.exger.2010.01.006

51. Gredilla R, Grief J, Osiewacz HD. Mitochondrial free radical generation and lifespan control in the fungal aging model *Podospora anserina. Exp Gerontol.* 2006;41(4):439-447. doi:10.1016/j.exger.2006.01.010

52. Wittig I, Braun HP, Schägger H. Blue native PAGE. *Nat Protoc.* 2006;1(1):418-428. doi:10.1038/nprot.2006.62

53. Heinz D, Krotova E, Hamann A, Osiewacz HD. Simultaneous ablation of the catalytic AMPK alpha-subunit SNF1 and mitochondrial matrix protease CLPP results in pronounced lifespan extension. *Front Cell Dev Biol.* 2021;9:616520. doi:10.3389/fcell.2021.616520

54. Pfaffl MW. A new mathematical model for relative quantification in real-time RT-PCR. *Nucleic Acids Res.* 2001;29(9):e45. doi:10.1093/nar/29.9.e45

55. Warnsmann V, Hainbuch S, Osiewacz HD. Quercetin-induced lifespan extension in *Podospora anserina* requires methylation of the flavonoid by the O-Methyltransferase PaMTH1. *Front Genet.* 2018a;9:160. doi:10.3389/fgene.2018.00160

56. Munoz-Gomez SA, Wideman JG, Roger AJ, Slamovits CH. The origin of mitochondrial cristae from alphaproteobacteria. *Mol Biol Evol.* 2017;34(4):943-956. doi:10.1093/molbev/msw298

57. Pfanner N, van der Laan M, Amati P, et al. Uniform nomenclature for the mitochondrial contact site and cristae organizing system. *J Cell Biol.* 2014;204(7):1083-1086. doi:10.1083/jcb.201401006

58. Bohnert M, Zerbes RM, Davies KM, et al. Central role of Mic10 in the mitochondrial contact site and cristae organizing system. *Cell Metab.* 2015;21(5):747-755. doi:10.1016/j.cmet.2015.04.007

59. Darshi M, Mendiola VL, Mackey MR, et al. ChChd3, an inner mitochondrial membrane protein, is essential for maintaining crista integrity and mitochondrial function. *J Biol Chem.* 2011;286(4):2918-2932. doi:10.1074/jbc.M110.171975

60. Li H, Ruan Y, Zhang K, et al. Mic60/Mitofilin determines MICOS assembly essential for mitochondrial dynamics and mtDNA nucleoid organization. *Cell Death Differ.* 2016;23(3): 380-392. doi:10.1038/cdd.2015.102

61. Stephan T, Brüser C, Deckers M, et al. MICOS assembly controls mitochondrial inner membrane remodeling and crista junction redistribution to mediate cristae formation. *EMBO J.* 2020;39(14):e104105. doi:10.15252/embj.2019104105

62. Opalinska M, Parys K, Janska H. Identification of physiological substrates and binding partners of the plant mitochondrial protease FTSH4 by the trapping approach. *Int J Mol Sci.* 2017;18(11):2455. doi:10.3390/ijms18112455

63. Yoon W, Hwang SH, Lee SH, Chung J. *Drosophila* ADCK1 is critical for maintaining mitochondrial structures and functions in the muscle. *PLoS Genet.* 2019;15(5):e1008184. doi:10.1371/journal.pgen.1008184

64. Schreiner B, Westerburg H, Forne I, Imhof A, Neupert W, Mokranjac D. Role of the AAA protease Yme1 in folding of proteins in the intermembrane space of mitochondria. *Mol Biol Cell.* 2012;23(22):4335-4346. doi:10.1091/mbc.E12-05-0420

65. Brust D, Daum B, Breunig C, Hamann A, Kühlbrandt W, Osiewacz HD. Cyclophilin D links programmed cell death

and organismal aging in *Podospora anserina*. *Aging cell*. 2010;9(5):761-775. doi:10.1111/j.1474-9726.2010.00609.x

66. Alkhaja AK, Jans DC, Nikolov M, et al. MINOS1 is a conserved component of mitofilin complexes and required for mitochondrial function and cristae organization. *Mol Biol Cell*. 2012;23(2):247-257. doi:10.1091/mbc.E11-09-0774

67. Anand R, Kondadi AK, Meisterknecht J, et al. MIC26 and MIC27 cooperate to regulate cardiolipin levels and the landscape of OXPHOS complexes. *Life Sci Alliance*. 2020;3(10). doi:10.26508/lsa.202000711

68. Anand R, Strecker V, Urbach J, Wittig I, Reichert AS. Mic13 is essential for formation of crista junctions in mammalian cells. *PLoS One*. 2016;11(8):e0160258. doi:10.1371/journal.pone.0160258

69. Beregi E, Regius O, Huttl T, Gobl Z. Age-related changes in the skeletal muscle cells. *Z Gerontol*. 1988;21(2):83-86.

70. Brandt T, Mourier A, Tain LS, Partridge L, Larsson NG, Kühlbrandt W. Changes of mitochondrial ultrastructure and function during ageing in mice and *Drosophila*. *eLife*. 2017;6:e24662. doi:10.7554/eLife.24662

71. Crane JD, Devries MC, Safdar A, Hamadeh MJ, Tarnopolsky MA. The effect of aging on human skeletal muscle mitochondrial and intramyocellular lipid ultrastructure. *J Gerontol A Biol Sci Med Sci*. 2010;65(2):119-128. doi:10.1093/gerona/glp179

72. McQuibban GA, Lee JR, Zheng L, Juusola M, Freeman M. Normal mitochondrial dynamics requires rhomboid-7 and affects *Drosophila* lifespan and neuronal function. *Curr Biol*. 2006;16(10):982-989. doi:10.1016/j.cub.2006.03.062

73. Scheckhuber CQ, Erjavec N, Tinazli A, Hamann A, Nyström T, Osiewacz HD. Reducing mitochondrial fission results in increased life span and fitness of two fungal ageing models. *Nat Cell Biol*. 2007;9(1):99-105. doi:10.1038/ncb1524

74. Young LC, Bone KM, Wang P, et al. Fusion tyrosine kinase NPM-ALK deregulates MSH2 and suppresses DNA mismatch repair function novel insights into a potent oncoprotein. *Am J Pathol*. 2011;179(1):411-421. doi:10.1016/j.ajpath.2011.03.045

75. Zhao L, Zou X, Feng Z, et al. Evidence for association of mitochondrial metabolism alteration with lipid accumulation in aging rats. *Exp Gerontol*. 2014;56:3-12. doi:10.1016/j.exger.2014.02.001

76. Warnsmann V, Meyer N, Hamann A, Kögel D, Osiewacz HD. A novel role of the mitochondrial permeability transition pore in (-)-gossypol-induced mitochondrial dysfunction. *Mech Ageing Dev*. 2018b;170:45-58. doi:10.1016/j.mad.2017.06.004

77. Yu R, Cao X, Sun L, et al. Inactivating histone deacetylase HDA promotes longevity by mobilizing trehalose metabolism. *Nat Commun*. 2021;12(1):1981. doi:10.1038/s41467-021-22257-2

78. Zerbes RM, Höß P, Pfanner N, van der Laan M, Bohnert M. Distinct roles of Mic12 and Mic27 in the mitochondrial contact site and cristae organizing system. *J Mol Biol*. 2016;428(8):1485-1492. doi:10.1016/j.jmb.2016.02.031

79. Kondadi AK, Anand R, Hansch S, et al. Cristae undergo continuous cycles of membrane remodelling in a MICOS-dependent manner. *EMBO Rep*. 2020;21(3):e49776. doi:10.15252/embr.201949776

80. Kanki T, Kang D, Klionsky DJ. Monitoring mitophagy in yeast: the Om45-GFP processing assay. *Autophagy*. 2009;5(8):1186-1189.

81. Meiling-Wesse K, Barth H, Thumm M. Ccz1p/Aut11p/Cvt16p is essential for autophagy and the cvt pathway. *FEBS Lett*. 2002;526(1-3):71-76.

82. Guo X, Zhang W, Wang C, et al. IRGM promotes the PINK1-mediated mitophagy through the degradation of Mitofilin in SH-SY5Y cells. *FASEB J*. 2020;34(11):14768-14779. doi:10.1096/fj.202000943RR

83. Wang LJ, Hsu T, Lin HL, Fu CY. Drosophila MICOS knockdown impairs mitochondrial structure and function and promotes mitophagy in muscle tissue. *Biol Open*. 2020;9(12), bio054262 doi:10.1242/bio.054262.

84. Graef M, Nunnari J. Mitochondria regulate autophagy by conserved signalling pathways. *EMBO J*. 2011;30(11):2101-2114. doi:10.1038/emboj.2011.104

85. Lee J, Giordano S, Zhang J. Autophagy, mitochondria and oxidative stress: cross-talk and redox signalling. *Biochem J*. 2012;441(2):523-540. doi:10.1042/BJ20111451

86. John GB, Shang Y, Li L, et al. The mitochondrial inner membrane protein mitofilin controls cristae morphology. *Mol Biol Cell*. 2005;16(3):1543-1554. doi:10.1091/mbc.e04-08-0697

87. Munkres KD. Histochemical detection of superoxide radicals and hydrogen peroxide by Age-1 mutants of *Neurospora*. *Fungal Genet Newsl*. 1990;37:24-25.

88. Merry TL, Ristow M. Mitohormesis in exercise training. *Free Radic Biol Med*. 2016;98:123-130. doi:10.1016/j.freeradbiomed.2015.11.032

89. Ristow M, Zarse K. How increased oxidative stress promotes longevity and metabolic health: the concept of mitochondrial hormesis (mitohormesis). *Exp Gerontol*. 2010;45(6):410-418. doi:10.1016/j.exger.2010.03.014

90. Maglioni S, Schiavi A, Runci A, Shaik A, Ventura N. Mitochondrial stress extends lifespan in *C. elegans* through neuronal hormesis. *Exp Gerontol*. 2014;56:89-98. doi:10.1016/j.exger.2014.03.026

91. Rea SL, Ventura N, Johnson TE. Relationship between mitochondrial electron transport chain dysfunction, development, and life extension in *Caenorhabditis elegans*. *PLoS Biol*. 2007;5(10):e259. doi:10.1371/journal.pbio.0050259

92. Schiavi A, Maglioni S, Palikaras K, et al. Iron-starvation-induced mitophagy mediates lifespan extension upon mitochondrial stress in *C. elegans*. *Curr Biol*. 2015;25(14):1810-1822. doi:10.1016/j.cub.2015.05.059

93. Cocheme HM, Murphy MP. Complex I is the major site of mitochondrial superoxide production by paraquat. *J Biol Chem*. 2008;283(4):1786-1798. doi:10.1074/jbc.M708597200

94. Wiemer M, Osiewacz HD. Effect of paraquat-induced oxidative stress on gene expression and aging of the filamentous ascomycete *Podospora anserina*. *Microb Cell*. 2014;1(7):225-240. doi:10.15698/mic2014.07.155

95. Callegari S, Dennerlein S. Sensing the stress: a role for the UPR(mt) and UPR(am) in the quality control of mitochondria. *Front Cell Dev Biol*. 2018;6(31):31. doi:10.3389/fcell.2018.00031

96. Hill S, Van Remmen H. Mitochondrial stress signaling in longevity: a new role for mitochondrial function in aging. *Redox Biol*. 2014;2:936-944. doi:10.1016/j.redox.2014.07.005

97. Kim HE, Grant AR, Simic MS, et al. Lipid biosynthesis coordinates a mitochondrial-to-cytosolic stress response. *Cell.* 2016;166(6):1539-1552.e1516. doi:10.1016/j.cell.2016.08.027

98. Tan JX, Finkel T. Mitochondria as intracellular signaling platforms in health and disease. *J Cell Biol.* 2020;219(5): e202002179. doi:10.1083/jcb.202002179

99. Wiedemann N, Pfanner N. Mitochondrial machineries for protein import and assembly. *Annu Rev Biochem.* 2017;86: 685-714. doi:10.1146/annurev-biochem-060815-014352

100. Körner C, Barrera M, Dukanovic J, et al. The C-terminal domain of Fcj1 is required for formation of crista junctions and interacts with the TOB/SAM complex in mitochondria. *Mol Biol Cell.* 2012;23(11):2143-2155. doi:10.1091/mbc.E11-10-0831

101. Aaltonen MJ, Friedman JR, Osman C, et al. MICOS and phospholipid transfer by Ups2-Mdm35 organize membrane lipid synthesis in mitochondria. *J Cell Biol.* 2016;213(5): 525-534. doi:10.1083/jcb.201602007

102. Serricchio M, Vissa A, Kim PK, Yip CM, McQuibban GA. Cardiolipin synthesizing enzymes form a complex that interacts with cardiolipin-dependent membrane organizing proteins. *Biochim Biophys Acta Mol Cell Biol Lipids.* 2018;1863(4):447-457. doi:10.1016/j.bbalip.2018.01.007

103. Marschall LM, Warnsmann V, Meeßen AC, Löser T, Osiewacz HD. Lifespan extension of *Podospora anserina* Mic60-subcomplex mutants depends on cardiolipin remodeling. *Int J Mol Sci.* 2022;23(9). doi:10.3390/ijms23094741

SUPPORTING INFORMATION

Additional supporting information can be found online in the Supporting Information section at the end of this article.